OPTICAL S-R FLIP-FLOP USING DARK-BRIGHT SOLITON CONVERSION CONTROL

SAYSAMONE SOYSOUVANH

A THESIS SUBMITTED IN PARTIAL FULFILLMENT
OF THE REQUIREMENT FOR THE DEGREE OF
MASTER OF ENGINEERING IN COMPUTER ENGINEERING
INTERNATIONAL COLLEGE
KING MONGKUT'S INSTITUTE OF TECHNOLOGY LADKRABANG
2012

KMITL – 2012 – IC – M – 006 - 005

Thesis Title	Optical S-R Flip-Flop Using Dark-Bright Soliton Conversion Control
Student	Mr. Saysamone Soysouvanh
Student ID	53601151
Degree	Master of Engineering
Program	Computer Engineering
Year	2012
Thesis Advisor	Assoc. Prof. Dr. Somsak Mitatha
Thesis Co-Advisor	Assoc. Prof. Noriyuki Komine
	Prof. Dr. Masahiro Yoshida

ABSTRACT

This thesis presents the study of a microring resonator system for optical S-R flip-flop by using dark-bright soliton conversion control within the all-optical add/drop filter devices. The optical soliton that exhibits very powerful and remarkable behaviors is used to perform the optical logic NAND gate and optical S-R flip-flop. In operation, all-optical data input logic "0" is formed by the dark soliton pulse and input data logic "1" is formed by the bright soliton pulse, respectively. The dark-bright soliton conversion behavior can be obtained and formed the logic pulses by a $\pi / 2$ phase shifted device, i.e. an optical add/drop filter (AD) which is composed of two set straight waveguides shaped to microring resonator.

By using the proposed system, the binary logic operation can be formed simultaneously at the through and drop ports, respectively. The obtained outputs logic "0" and logic "1" are represented by dark and bright solitons respectively. In the optical S-R flip-flop application can be recognized as a simple and flexible system for forming the logic switching system. Numerical simulation results are obtained and confirmed for the useful application, in which the advanced logical system can be operated.

ACKNOWLEDGEMENTS

This thesis has been done completely by the attention in advising of advisor and co-advisors. The author would like to give the acknowledge to Assoc. Prof. Dr. Somsak Mitatha who is the thesis advisor of this thesis, the author would also like to thank Assoc. Prof. Noriyuki Komine and Prof. Dr. Masahiro Yoshida who is the thesis co-advisors from Tokai University, JAPAN for giving the useful knowledge, many invaluable experiences, research methodologies all the time during the period time of 2 years at King Mongkut's Institute of Technology Ladkrabang (KMITL).

The author would like to thank every encouragement especially from parents and family for supporting in any higher education and going abroad. Thank for many helps from the seniors for the advice and encouragement and using life time together for 2 years at the Hybrid Computing Research Laboratory (HCRL) and the Nanoscale Science and Engineering Research Alliance (N'SERA) Laboratory.

I would also like to thank my organization (NUOL) for giving me a change for going abroad to KMITL, Thailand. This change can give me a valuable experience for improving and growing myself.

And I would also like to thank friends, coworkers including other people that could not be listed all of the names in this thesis. The author would like to thank very much for this opportunity.

Finally, the author would like to thank the International College and the King Mongkut's Institute of Technology Ladkrabang for being the host institution for my favorite major i.e. computer engineering.

Oct 01, 2012

Saysamone Soysouvanh

TABLE OF CONTENTS

LIST OF FIGURES

LIST OF TABLES

Chapter 1

Introduction

1.1 Motivation

The electrical signal processing was anticipated to confront with the speed and bandwidth limitation in the near future, due to such problems, the researchers have researched and found the powerful tool and application to overcome such problems and the optical signal processing has become such a tool. To date, the studies of optical techniques have been widely increasing and applying into many applications for higher speed and proficient systems, one of those applications is an optical signal processing system.

In optics, the optical signal processing has been increasing remarkably. Many researches have demonstrated various logic or processing system for optical logic gates and optical flip-flop operations based on various schematics of optical signal processing, i.e. a terahertz optical asymmetric demultiplexer (TOAD) [1, 2], semiconductor optical amplifier (SOA) [3, 4], nonlinear effects in silicon-on insulator (SOI) waveguide [5], nonlinear loop mirror [6], DPSK format [7], local nonlinear in Mach-Zehnder interferometer (MZI) [8], Fabry-Perot laser diode [9], ring lasers [10], photonic crystals [11-13], DBR laser diode [14] have been proposed, many proposed works are still complex, however the search of more simple and flexible design system still remains.

Nowadays, optical flip-flop is an essential component of latching functions in ultra high speed all-optical processing applications [15, 16]. For this concept, the optical S-R flip-flop operation of binary based on dark-bright solitons conversion behaviors can be performed, in which the coincidence of dark and bright soliton pulses can be separated after propagating into the optical filter device with $\pi/2$ phase shifted (an optical channel dropping filter) [17]. The proposed scheme is based on a 1 bit binary to the complex logic circuits, which can be compared by any two bits when logic '0' and '1' are formed by dark soliton (D) and bright soliton (B), respectively.

1.2 Scope of the Thesis

In this thesis proposes an optical S-R flip-flop schematic based on dark-bright solitons conversion control. Within a $\pi/2$ phase shift optical add/drop device, the dark-bright solitons collision behavior is performed and obtained at the through and drop ports of the add/drop filter device. When the output of the through port is a bright soliton (B) then the output of the drop port is a dark soliton (D), in another way, if a bright soliton is obtained at the drop port, then a dark soliton is obtained at the through port.

We assume that data logic 0 is represented by dark soliton and data logic 1 is represented by bright soliton, respectively, then the optical logic NAND gate can be performed by using dark-bright solitons conversion control techniques [18, 19]. Only the optical logic NAND gate is presented in this thesis. Moreover, the optical S-R flip-flop operation can be designed and simulated.

Finally, the new design system for optical S-R flip-flop based on dark-bright solitons conversion control within a $\pi/2$ phase shift optical device i.e. add/drop filter is proposed and simulated.

1.3 Expected Results

The principle objective of the thesis is studying and understanding the dark-bright solitons conversion technique within an optical add/drop filter device, the theoretical background which can be used to perform the system design for optical logic gates and optical S-R flip-flop based on dark-bright solitons conversion control for higher speed optical logic processing applications.

In this thesis proposes an all-optical S-R flip-flop system for logical processing operation which can be replaced use for an electronic circuit [20, 21]. By using dark-bright solitons conversion control concept within the add/drop filter. The expected of the proposed system is to obtain a simple and flexible system within the minimum loss for optical logic signal processing with high speed communication, the system can be performed the high speed logic transmission and obtained the result instantly.

1.4 Organization of the Thesis

Chapter 1 – Introduction: In this chapter outlines the introduction of basic background in the research area, the recent works and the literature of the related research works, and the incentive to do this thesis, the scope and the expected result of the work are also included.

Chapter 2 – Literature Reviews and Theoretical backgrounds: In this chapter outlines the basic theory backgrounds of the linearity-nonlinearity optical communication, the all-optical technique named as dark-bright soliton conversion control within a passive optical device. The optical ring resonator and its mathematical modeling, the generation of optical add/drop filter and its mathematical modeling, the phenomena that occur in such add/drop filter that can be used to perform the optical logic gates and optical S-R flip-flop and the literatures of the related works are also reviewed in this chapter.

Chapter 3 – Optical logic NAND gate using dark-bright soliton conversion control: In this chapter outlines the structure and schematic of the optical NAND gate based on dark-bright solitons conversion behavior within the optical add/drop filter, the simulation and the result of the experiment and discussion.

Chapter 4 – Optical S-R flip-flop using dark-bright soliton conversion control: In this chapter outlines the schematic of novel optical S-R flip-flop based on dark-bright soliton conversion techniques within the optical add/drop filters, the simulation and the result of the system, and the discussion.

Chapter 5 – Conclusion: In this chapter, the conclusion of the proposed work, the outlines of the advantages and disadvantages of recently proposed work, the probability to make an improvement of such a design system in the near future, the suggestions for future works related to this research are given as well.

Chapter 2

Literature Reviews and Theoretical Backgrounds

2.1 Literature Reviews

The electrical signal processing is the techniques used to perform the logical operations i.e. logical gates, flip-flops, etc. such all operations are used in electronic devices, due to the increasing of speed and bandwidth requirement of the system in the near future, but the electrical signal processing was anticipated to be not able to respond in such requirements, the researchers have researched and demonstrated that the optical signal processing is the powerful tool and application to overcome such problems of the electrical signal processing. To date, the studies of optical techniques have been widely increasing, many researches have demonstrated the replacement used and applying into many applications for higher speed and proficient systems, instead of the electrical signal processing system [20, 21, 54, 55].

Since the last decade, optical signal processing has increased remarkably, many schemes can perform the processing system in a form of optical logic processing, by using different methods, the optical logic gates and optical flip-flops can be performed. The proposed of the optical gates and optical flip-flop using various schemes of the optical signal processing techniques have been demonstrated. In this section the literatures of the optical logic gate and optical flip-flop are reviewed.

2.1.1 All-Optical Logic Gate using an Add-Drop Filter and Intensity Switch

Thananchai Threepak et al. [22] has designed a system composed of two components, an add-drop optical filter and an intensity switch. In this system, an add-drop optical filter is used to combine two Gaussian laser pulses. By organizing coupling coefficient value, both input signals from Add port and E_{in} port are summed up and produce results at the $E_{through}$ port. Afterward, an intensity switch is used to split high intensity signal to the P_{out1} port and low intensity signal to the P_{out2} port. To regulate separation method, the authors can adjust the compensated angle of the signal line and surface of nonlinear material in intensity switch.

To design the intensity switch, they exercise two theories of nonlinear optics. First, when light propagates within the nonlinear material (medium), the refractive index (n) of light within the medium is given by: $n = n_0 + n_2 I = n_0 + \left(n_2 / A_{eff}\right) P$, where n_0 and n_2 are the linear and nonlinear refractive indexes, respectively. I and P are the optical intensity and optical power, respectively. The effective mode core area of the device is given by A_{eff}. By using this theory, they can change reflective index of nonlinear material using intensity.

Second, the nonlinear law of reflection [23] allows any signals to reflect and refract at the surface of nonlinear material. By using this theory, they can produce a light switching. Through these manners, they are able to create a device that can merge and split light pulse signals. This device can be used as a logic operation device, AND gate and inverter. Moreover, they can fabricate all optical switching devices or routers that operate in an optical layer.

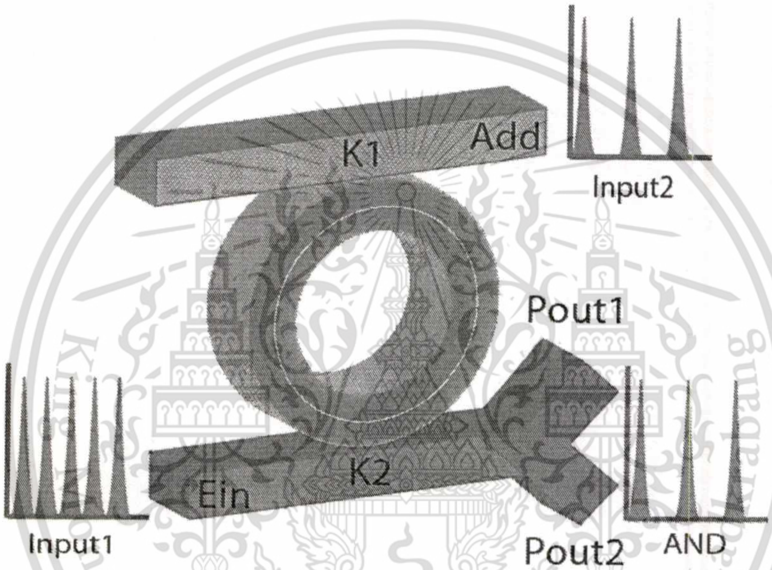

Fig. 2. 1 AND operation result

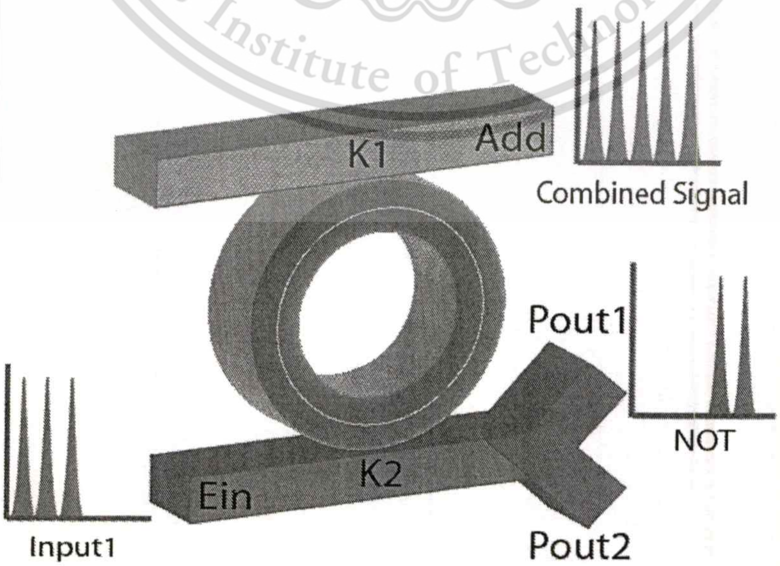

Fig. 2. 2 Inverter operation result

The authors simulated the designed system to produce AND [see Fig. 2.1] gate and inverter [see Fig. 2.2] by using add-drop optical filter and intensity switch. Ring resonator has $5\,\mu m$ radius. Coupling coefficient of Add/Drop part and $E_{in}/E_{throuth}$ are fixed to *K1* = 0.9 and *K2* = 0.1. Fractional coupler intensity loss on both sides of the ring are $\gamma = 0.1$. Waveguide ring resonator loss is $D = 0.06\,dBmm^{-1}$, and a lambda of waveguide is $1.2\,\mu m$. Intension switching composed of two nonlinear materials. First material has the linear reflective index equal to 1.8, and the nonlinear reflective index equal to $2.9\times10^{-16}\,m^2W^{-1}$. Second material has the linear reflective index equal to 1.5 and the nonlinear reflective index equal to $2.3\times10^{-10}\,m^2W^{-1}$.Laser pulse signals are generated at 13 *Gbps*.

2.1.2 Optical Flip-Flop Based on Two-Coupled Mode-Lock Ring Lasers

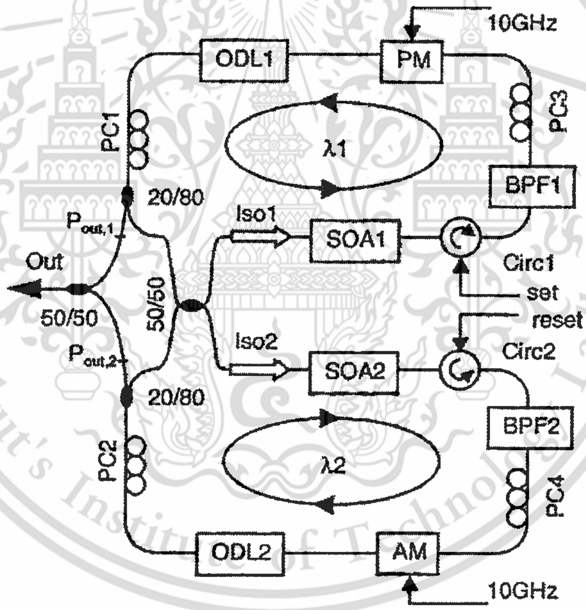

Fig. 2. 3 Schematic of optical flip-flop based on two coupled ring lasers. Circ: Optical Circulator.

In Fig. 2.3, Eduward Tangdiongga et al. [10], presented a schematic of the optical flip-flop. The system consists of two-coupled lasers operating at central wavelengths λ_1 and λ_2, respectively. Each cavity contains a phase or amplitude modulator (AM/PM), an optical delay line (ODL), an iusolator (Iso), a bandpass filter (BPF), a semiconductor optical amplifier (SOA), a circulator, and polarization controllers (PCs). The total length of each cavity was approximately 20 *m*. The authors used two bulk

In-GaAsP–InP SOAs with a $800\,\mu m$ long active region. The SOAs has an optimum gain at 1537 *nm* and 1547 *nm*, respectively, and they can provide 23 *dB* small-signal gain at a bias current of approximately 300 *mA*. In both ring cavities, the SOA exhibits a polarization sensitivity of 2 *dB*, while the polarization sensitivity of the AM and PM modules was 3-4 *dB*. The polarization dependencies were compensated by using PCs. The Iso's were used to ensure unidirectional leasing. The BPF [5 nm, full-width at half-maximum (FWHM)] defined the central wavelength of each cavity and the ODL was used to precisely match multiples of the cavity resonance frequency to the repetition rate. The total cavity loss was $10-13\,dB$ and its cavity fundamental frequency was $6.689\,MHz$. Note that there is no specific reason for using different modulators in the MLRLs. It is important, however, that the pulse widths and optical powers in each ring are identical to allow symmetric coupling.

The flip-flop operation was realized by symmetrically connecting the two cavities such that one laser acts as a master, suppressing the other laser, which consequently acts as a slave. The role of master and slave can be interchanged due to the system symmetry. Thus, the system has two states, depending on which laser is lasing. The state can be determined by the wavelength of the output light. To switch between the states, external light has to be injected into the master. The external light quenches the gain of the master so that lasing is stopped. The absence of light from the master laser allows the slave laser to start lasing to become the master. The flip-flop remains in the new state after the external light has been removed.

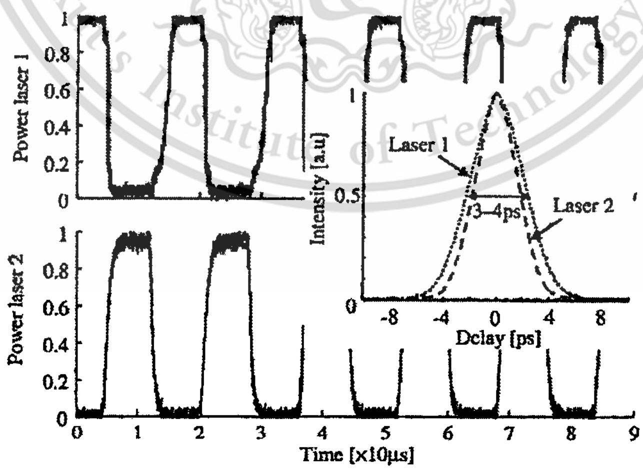

Fig. 2. 4 Regular switching between two flip-flop states as a result of the set–reset signal, the inset shows typical pulse shapes of the MLRLs. MLRL: mode-locked ring lasers.

The dynamic operation of the all-optical flip-flop (AOFF) was investigated by injecting a regular sequence amplitude modulated ones and zeroes in the laser that was currently the master. This causes the AOFF to change its state after a certain amount of time. The duration of each one and zero was $10\,s$, the central wavelength of this signal was $1551\,nm$, and the average power was $1\,mW$. The AOFF output was detected by a slow photo detector and displayed on an oscilloscope. Due to the limitation of the detector response time, Fig. 2.4 shows only the envelope of the picosecond pulse train. It should be noted, however, that each one-state consists of a sequence of optical pulses with duration of $3-4\,ps$ (see inset) at a repetition rate of $10\,GHz$. They found that the flip-flop could change state in less than $2\,s$ (see the risetime-falltime in Fig. 2.4). This implies that pulses can build up after about $20-30$ round-trip times.

2.2 Theoretical Background

The study of light pulse propagation along the dielectric (nonlinear) media is the phenomena of light which is due either to the changes in refractive index with optical power or the scattering phenomena. The power dependence of refractive index is responsible for the Kerr effect. Nonlinear optics is the study of phenomena that occur as a consequence of the modification of the optical properties of a material under intense illumination. Typically, only laser light is sufficiently intense to modify the optical properties of a material.

Depending on the shape of the input signal, the Kerr nonlinearity appears itself by different effects, such as self-phase modulation, cross-phase modulation, nonlinear behaviors of light travelling in fiber optics are commonly induced by the effects such as Kerr effects [30], four-wave mixing [31], and the external nonlinear pumping power [32]. The nonlinear behaviors occur are named as chaos, bistability and bifurcation [33], the details of such behaviors of light travelling in a microring resonator are clearly described by Yupapin [34].

When light propagates within the nonlinear material (media), the refractive index (n) of light within the medium is given by Eq. 2.1

$$n = n_0 + n_2 I = n_0 + \left(\frac{n_2}{A_{eff}}\right) P \qquad \text{(Eq. 2.1)}$$

Where n_0 and n_2 are the linear and nonlinear refractive indexes, respectively. I is the optical intensity and P is the optical power. The effective mode core area of the device is A_{eff}.

2.2.1 Optical Soliton

In a linear medium, the phase between the different plane waves depends solely on the propagation angle. It is clear then, that if all the plane wave components have the same angles, they will also have the same phase velocity and no phase difference will be acquired during propagation. If we represent the propagation direction of these plane waves by arrows, these arrows will create a cone in space. The associated beam will propagate in this linear medium with no broadening while it maintains its shape and dimensions. This type of beams is called "Bessel beams" since their field is described by Bessel function.

In a nonlinear medium, however, each plane wave is influenced by all the others. This is because the index change is a function of the total intensity. For some nonlinear cavities it is possible to find an ensemble of plane waves which will delay the phase velocity of the on axis components (in comparison with the off axis components) Consequently, the phase delay between the different propagating plane waves (explained in the previous section) will be compensated by the other waves via the medium nonlinearity.

If the nonlinearity is such that the index at the beam center is higher than in the dark regions, then the plane wave that propagates on the axis will experience the highest index and will propagate slower from those off axis. This high index experienced by the on axis wave can compensate for its linear tendency to propagate faster (because it is the on axis). One example in which the index of refraction fully compensates for the shorter trajectory is a hyperbolic secant solution in a Kerr type medium. The plane waves that construct the hyperbolic secant index profile (induced by the beam via the nonlinearity) have all the same phase velocity along propagation, and hence their interference (the hyperbolic secant shape) also maintains its shape and size as it propagates.

One can also look on soliton from the mathematical perspective. One has to find a stationary wave solution of governing nonlinear wave equation. The mathematical aspects of the soliton are out of the scope of this thesis. Hence, here I will give just the final solution. For the exact mathematical derivation, the reader may refer to [35-36].

2.2.2 Dark and Bright Solitons

Optical soliton has become a powerful tool that can overcome the problems of using Gaussian pulse such as the limit of laser power can cause a problem, especially when the high output power or long distance link is required, the use of soliton pulse can fix a such problem i.e., a high power laser source. Furthermore, the non-dispersion of soliton in medium is the other advantage. Optical soliton can be naturally divided into classes of dark soliton and bright soliton as shown in Fig. 2.5 (a) and (b) respectively.

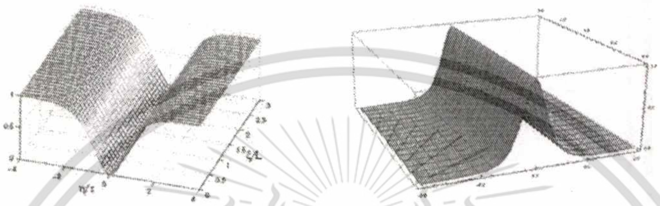

(a) Dark soliton *(b) Bright soliton*

Fig. 2. 5 Dark and bright soliton pulses

A dark soliton pulse exhibits an interesting and remarkable behavior, especially when it is transmitted into an optical transmission system. It has the advantage of the signal detection difficulty, when the ambiguity of signal detection becomes a problem for the un-wanted users. In principle, the soliton generation and their behaviors in media are well analyzed and described by Agarwal [37]. Many earlier theoretical and experimental works on soliton applications can be found in the soliton application book by Hasegawa [38]. However, to make such a tool more useful, the problems of soliton-soliton interactions [39], collision [40], rectification [41], and dispersion management [42] must be solved and addressed.

The function of dark and bright solitons are given by Eq. 2.2 and Eq. 2.3 respectively [37]

$$E_{dark}(t) = A.tanh\left[\frac{T}{T_0}\right] exp\left[\left(\frac{z}{2L_D}\right) - i\omega_0 t\right] \quad \text{(Eq. 2.2)}$$

$$E_{bright}(t) = A.sech\left[\frac{T}{T_0}\right] exp\left[\left(\frac{z}{2L_D}\right) - i\omega_0 t\right] \quad \text{(Eq. 2.3)}$$

Where A is the optical field amplitude, z is the propagation distance, T is a soliton pulse propagation time in a frame moving at the group velocity, where ($T = t - \beta_1 z$), β_1 and β_2 are the coefficients of the linear and second-order terms of Taylor expansion of the propagation constant respectively, L_D is the dispersion length of the soliton pulse ($L_D = T_0^2/|\beta_2|$), T_0 is a soliton pulse propagation time of initial input (or soliton pulse width), t is the soliton phase shift time, ω_0 is the frequency shift of the soliton.

For the soliton pulse in the microring device, a balance should be achieved between the dispersion length (L_D) and the nonlinear length ($L_{NL} = 1/\Gamma\phi_{NL}$), where $\Gamma = n_2 k_0$ is the length scale over which dispersive or nonlinear effects make the beam become wider or narrower. For a soliton pulse, there is a balance between dispersion and nonlinear lengths, hence $L_D = L_{NL}$.

2.3 Ring Resonator

The proposed research to use an integrated ring resonator for a bandwidth pass filter has been first made since 1969 by E. A. J. Marcatili [43] and the transmission properties of the use waveguide consisting of a dielectric rod with rectangular cross section, surrounded by several dielectrics of smaller refractive indices have been described by E. A. Marcatili [44]. In the research area of nonlinear media, the materials such as $GaAs$ and InP [45, 46] are the great interesting for the researchers in the last several decades due to the higher nonlinear coefficients than other materials, these materials can be designed as a waveguide to conducing the optical signal or laser in a wavelength of $1550\ nm$ [47] for applied to other applications.

A general architecture for an autoregressive planar waveguide optical filter was demonstrated for the first time in 1996 [48]. The schematic of a ring resonator channel dropping filter is as shown in Fig. 2.10. The autoregressive lattice filters which were designed and fabricated consisted of one and two stages using Ge-doped silica waveguides.

Purely passive single coupler ring resonator filter (SSR) as shown in Fig. 2.6 has been realized in the materials system i.e. $AlGaAs - GaAs$ [49], $Si - SiO_2$ [50] and $Si_3N_4SiO_2$ [51]. The radius of the used ring resonator is between $5\ \mu m$ and $30\ \mu m$ and the free spectral range (FSR) achieved is between $20\ nm$ and $30\ nm$. Passive ring resonators in the form of a racetrack have been realized in the material system $GaInAsP$ [52] and $AlGaAs - GaAs$ [53]. The performances of those filters are limited by bending and scattering losses in the resonator. These losses could be compensated by using an active material instead or in addition.

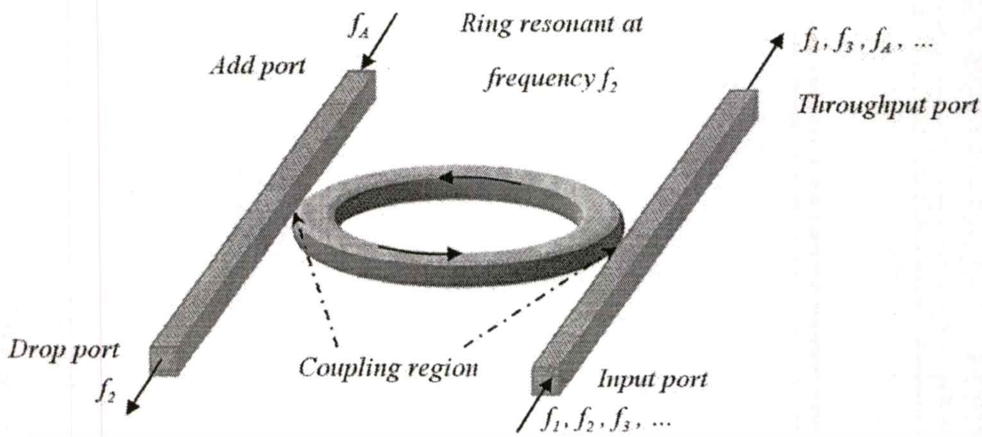

Fig. 2. 6 Ring resonator channel dropping filter

2.3.1 Single Coupled Ring Resonator

A single coupled ring resonator is simply a waveguide shaped into a closed loop ring waveguide at the coupling point. The ring structure is shown in Fig. 2.11. To determine optical filter transfer function in Z-domain, the requirements of optical filters are considered to be satisfied as: linearity of all optical components, time invariance of all optical components, and optical components must be lumped (i.e. not distributed)

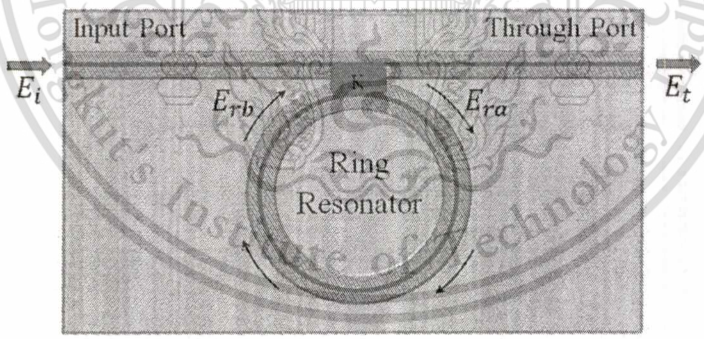

Fig. 2. 7 Structure of the single coupled ring resonator

Where E_i is the input field into input port,

E_t is throughput field transmitting at throughput port,

The effects such as backscatter of light along the length of an optical fiber or waveguide, or saturation of an optical amplifier is therefore not considered here (the former is a distributed phenomenon; the latter is a nonlinear effect).

2.3.2 Mathematical Model of Single Coupled Ring Resonator

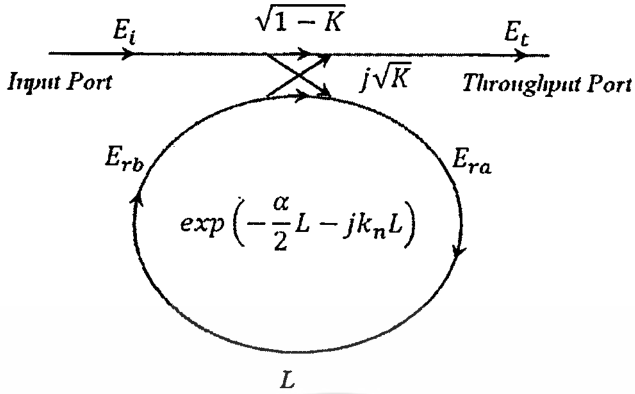

Fig. 2. 8 Schematic diagram of single coupled ring resonator

The transfer function of this configuration is derived by using Z-transform analysis. The Z-transform parameter is represented by: $z^{-1} = exp^{-jk_nL}$,

Where k_n is the propagation constant ($k_n = \frac{2\pi}{\lambda} n_{eff}$),

n_{eff} is the effective index of the waveguide,

a is the one round trip loss ($a = exp^{-\frac{\alpha}{2}L}$),

α is the intensity attenuation coefficient inside the waveguide (unit *length*$^{-1}$)

L is the circumference of the ring resonator waveguide ($L = 2\pi R$),

K is the coupling coefficient between the ring and the straight waveguide

The transmitted or throughput field at the throughput port of the Single coupler ring resonator is E_t, and input field is E_i, the relations can be derived as equations below:

$$E_t = (1-\gamma)^{1/2}.\left[E_i\sqrt{1-K} + jE_{rb}\sqrt{K}\right] \quad \text{(Eq. 2.4)}$$

$$E_{ra} = (1-\gamma)^{1/2}.\left[jE_i\sqrt{K} + E_{rb}\sqrt{1-K}\right] \quad \text{(Eq. 2.5)}$$

$$E_{rb} = E_{ra}.exp^{-\frac{\alpha}{2}L}.exp^{-jK_nL} = E_{ra}.a.z^{-1} \quad \text{(Eq. 2.6)}$$

Using the equations above: hence, E_t/E_i can be calculated by:

$$\frac{E_t}{E_i} = (1-\gamma)^{1/2}.\left[\frac{\sqrt{1-K}-(1-\gamma)^{1/2}.a.z^{-1}}{1-(1-\gamma)^{1/2}.\sqrt{1-K}.a.z^{-1}}\right] \quad \text{(Eq. 2.7)}$$

The transfer function in Eq. 2.7 indicates that a ring resonator is very similar to a Fabry-Perot cavity. In the particular case as shown in Fig. 2.9, the corresponding Fabry-Perot cavity would have an input mirror with a field reflectivity and a fully reflecting output mirror. However, the field propagating inside the ring cavity is a traveling wave in contrast to the Fabry-Perot cavity which resonates a standing wave, for simplification, new parameters are used in following:

$$D = (1-\gamma)^{1/2}$$
$$x = D.exp^{1-\frac{\alpha}{2}L}$$
$$y = \sqrt{1-K}$$
$$\emptyset = k_n.L \qquad \text{(Eq. 2.8)}$$

Hence, the intensity relation to the output port is given by:

$$T = \frac{I_t}{I_i}(\emptyset) = \left|\frac{E_t}{E_i}\right|^2 = D^2.\left[1 - \frac{(1-x^2).(1-y^2)}{(1-x.y)^2+4.x.y.sin^2\left(\frac{\emptyset}{2}\right)}\right] \qquad \text{(Eq. 2.9)}$$

The maximum and minimum of transmissions are calculated by:

$$T_{max} = D^2 \cdot \frac{(x+y)^2}{(1+x.y)^2} \qquad \text{(Eq. 2.10)}$$

$$T_{min} = D^2 \cdot \frac{(x-y)^2}{(1-x.y)^2} \qquad \text{(Eq. 2.11)}$$

The minimum transmission (T_{min}) occurs at the resonant point when the circumference of the ring (L) is an integral number of guide wavelength which defined by

$$\emptyset = k_n.L = 2m\pi$$
$$m.\lambda_m = n.L \qquad \text{(Eq. 2.12)}$$

Here, m is the mode number (m = integer), L_m is the resonant mode wavelength.

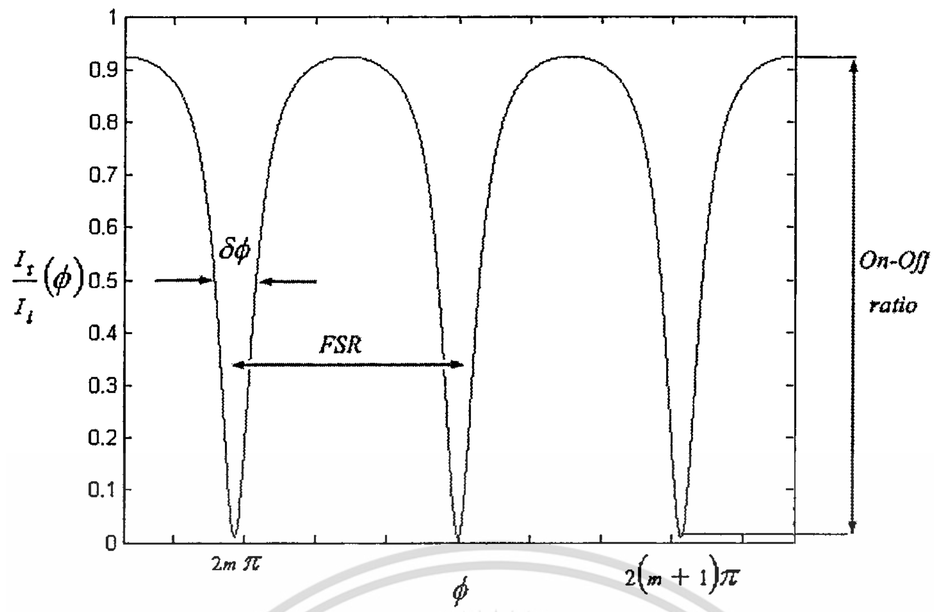

Fig. 2. 9 Transmission characteristic of a single coupled ring resonator

The on-off ratio for the through and drop ports, which is the ratio of the on-resonance intensity to the off- resonance intensity which is given by:

$$ON - OFF\ ratio = \frac{T_{\max(throughput\ port)}}{T_{\min(drop\ port)}} \quad \text{(Eq. 2.13)}$$

The on-off ratio will become maximum if

$$T_{\min} = 0 \Rightarrow x = y \Rightarrow \alpha = -\frac{1}{L} \cdot \ln(\frac{1-K}{D^2}) \quad \text{(Eq. 2.14)}$$

This relationship is also referred to as the critical coupling. The maximum on-off ratio ($\frac{I_t}{I_i}(2m\pi) = 0$), (Fig. 2.9) can be achieved by varying the coupling factor K or the intensity attenuation coefficient α (Eq. 2.14). The value of α can only be changed severely by the implementation of an SOA within the ring resonator or using an all-active ring resonator.

2.3.3 Double Coupled Ring Resonator (Add/Drop Filter)

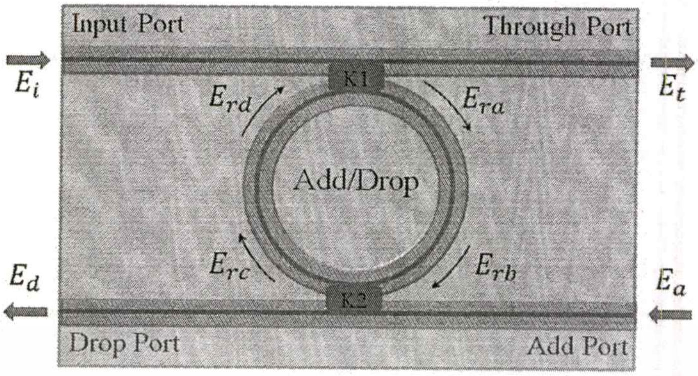

Fig. 2. 10 Structure of the add/drop filter

Where E_i is the electric field at the input port,

E_t is electric field at the through port,

E_a is the electric field at the add (control) port,

E_d is the electric field at drop port,

E_{ra} ... E_{rd} are the electric fields at points a ... d, respectively,

K_1, K_2 are the coupling coefficients

Double coupled ring resonator filter which is called add/drop filter is composed of two planar waveguide shaped to a closed loop waveguide. The loop can be any closed shape, such as a circle, ellipse, or race track. The ring is placed near one or two bus waveguides (Fig. 2.10). Typically, the input signal consists of one or more WDM channels. Signals on the input bus couple evanescently to the resonator. If a channel wavelength is resonant in the resonator, i.e., it encounters an integral multiple of 2π in phase over a round-trip, the signal intensity builds up in the ring, it is coupled to the output bus, and is "dropped." At the same time, a signal on the same wavelength can be added via the add port. The resonator thus functions as an optical add/drop multiplexer.

2.3.4 Mathematical Model of Add/Drop Filter

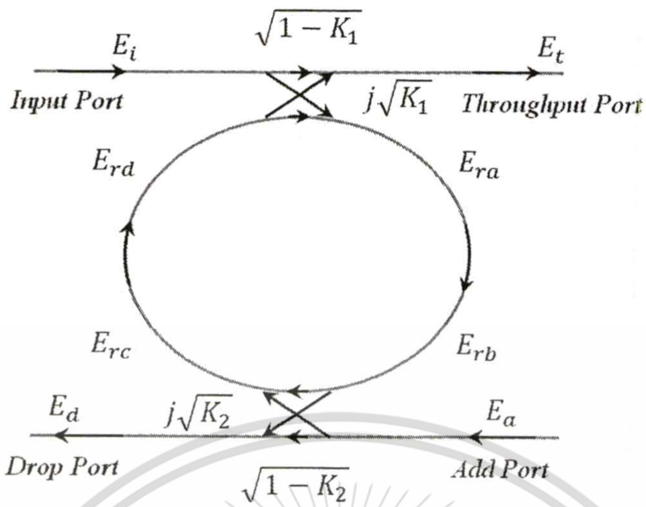

Fig. 2. 11 Schematic diagram of double couple ring resonator

Consider the architectures of an add/drop filters as illustrated in (Fig. 2.11), which are constructed by 2×2 optical couplers. Similarly, the optical transfer functions of the ring resonator filters at the throughput port and drop port for an input port E_i can be derived as follows, for the first coupling coefficient (K_1), we have

$$E_t = \sqrt{1-\gamma_1}\left[j\sqrt{K_1}E_{rd} + \sqrt{1-K_1}E_i\right] \quad \text{(Eq. 2.15)}$$

$$E_{ra} = \sqrt{1-\gamma_1}\left[j\sqrt{K_1}E_i + \sqrt{1-K_1}E_{rd}\right] \quad \text{(Eq. 2.16)}$$

Where γ_1 and K_1 are the coupling loss and the coupling coefficients, respectively. The incoming light of E_i and E_{rd} are coupled through the first coupling coefficient to the output light E_t and the output light E_{ra} is transmitted through the ring becomes output light (E_{rb}). According to the light transmission theory in linear optical systems, we obtain the following relation between E_{ra} and E_{rb}

$$E_{rb} = E_{ra}e^{-\frac{\alpha L}{2 2}-jk_n\frac{L}{2}} \quad \text{(Eq. 2.17)}$$

Where the transmission line length is $L/2$. The second coupling coefficient (K_2) has the following relations:

$$E_d = E_{ra} e^{-\frac{\alpha}{2}\frac{L}{2} - jk_n\frac{L}{2}} . j\sqrt{1-\gamma_2}\sqrt{K_2} \qquad \text{at } E_a = 0 \qquad \text{(Eq. 2.18)}$$

$$E_{rc} = E_{ra} e^{-\frac{\alpha}{2}\frac{L}{2} - jk_n\frac{L}{2}} . j\sqrt{1-\gamma_2}\sqrt{1-K_2} \qquad \text{(Eq. 2.19)}$$

Using the transmission theory, we obtain E_{rd} in terms of E_{rc}

$$E_{rd} = E_{rc} e^{-\frac{\alpha}{2}\frac{L}{2} - jk_n\frac{L}{2}} \qquad \text{(Eq. 2.20)}$$

$$E_{ra} = \frac{E_i j\sqrt{1-\gamma_1}\sqrt{K_1}}{1-\sqrt{1-\gamma_1}\sqrt{1-K_1}\sqrt{1-\gamma_2}\sqrt{1-K_2}\, e^{-\frac{\alpha}{2}L - jk_n L}} \qquad \text{(Eq. 2.21)}$$

$$E_{rd} = \frac{E_i j\sqrt{1-\gamma_1}\sqrt{K_1}}{1-\sqrt{1-\gamma_1}\sqrt{1-K_1}\sqrt{1-\gamma_2}\sqrt{1-K_2}\, e^{-\frac{\alpha}{2}L - jk_n L}} \sqrt{1-\gamma_2}\sqrt{1-K_2}\, e^{-\frac{\alpha}{2}L - jk_n L} \qquad \text{(Eq. 2.22)}$$

By using the upper equations, the transfer function for throughput port and drop port in (Fig. 2.11) can thus be expressed as

Throughput port:

$$\frac{E_t}{E_i} = \frac{-(1-\gamma_1)K_1\sqrt{1-K_2}\, e^{-\frac{\alpha}{2}L - jk_n L} + \sqrt{1-\gamma_1}\sqrt{1-K_1} - (1-\gamma_1)(1-K_1)\sqrt{1-\gamma_2}\sqrt{1-K_2}\, e^{-\frac{\alpha}{2}L - jk_n L}}{1-\sqrt{1-\gamma_1}\sqrt{1-K_1}\sqrt{1-\gamma_2}\sqrt{1-K_2}\, e^{-\frac{\alpha}{2}L - jk_n L}}$$

$$\frac{E_t}{E_i} = \frac{-\sqrt{1-\gamma_2}\sqrt{1-K_2}\, e^{-\frac{\alpha}{2}L - jk_n L} + \sqrt{1-\gamma_1}\sqrt{1-K_1}}{1-\sqrt{1-\gamma_1}\sqrt{1-K_1}\sqrt{1-\gamma_2}\sqrt{1-K_2}\, e^{-\frac{\alpha}{2}L - jk_n L}} \qquad \text{(Eq. 2.23)}$$

Drop port:

$$\frac{E_d}{E_i} = \frac{-\sqrt{1-\gamma_1}\sqrt{1-\gamma_2}\sqrt{K_1.K_2}\, e^{-\frac{\alpha}{2}L - jk_n L}}{1-\sqrt{1-\gamma_1}\sqrt{1-K_1}\sqrt{1-\gamma_2}\sqrt{1-K_2}\, e^{-\frac{\alpha}{2}L - jk_n L}} \qquad \text{(Eq. 2.24)}$$

The intensity relations for the throughput and drop port can be obtained by normalizing the transfer functions in (Eq. 2.23) and (Eq. 2.24) which are given by (Eq. 2.25) and (Eq. 2.26) as below

$$\frac{I_t}{I_i} = \left|\frac{E_t}{E_i}\right|^2 = \frac{-(1-\gamma_1)K_1 - 2\sqrt{1-\gamma_1}\sqrt{1-K_1}\sqrt{1-\gamma_2}\sqrt{1-K_2}\, e^{-\frac{\alpha}{2}L}\cos(k_n L) + (1-\gamma_2)(1-K_2)e^{-\alpha L}}{1+(1-\gamma_1)(1-K_1)(1-\gamma_2)(1-K_2)e^{-\alpha L} - 2\sqrt{1-\gamma_1}\sqrt{1-K_1}\sqrt{1-\gamma_2}\sqrt{1-K_2}\, e^{-\frac{\alpha}{2}L}\cos(k_n L)}$$

$$\frac{I_d}{I_i} = \left|\frac{E_d}{E_i}\right|^2 = \frac{(1-\gamma_1)(1-\gamma_2)K_1K_2e^{-\alpha L}}{1+(1-\gamma_1)(1-K_1)(1-\gamma_2)(1-K_2)e^{-\alpha L} - 2\sqrt{1-\gamma_1}\sqrt{1-K_1}\sqrt{1-\gamma_2}\sqrt{1-K_2}e^{-\frac{\alpha}{2}L}\cos(k_nL)}$$

(Eq. 2.25 and Eq. 2.26, respectively)

For simplification, the calculation of the intensity relation does not take into account coupling losses ($\gamma_1 = \gamma_2 = 0$) and the following parameters:

$$x = e^{-\frac{\alpha}{2}L}$$
$$c_1 = \sqrt{1-K_1}$$
$$c_2 = \sqrt{1-K_2} \qquad \text{(Eq. 2.27)}$$

The intensity relations Eq. 2.25 and Eq. 2.26 are then given by

$$\frac{I_t}{I_i}(\phi) = \left|\frac{E_t}{E_i}\right|^2 = 1 - \frac{(1-c_1^2)\cdot(1-c_1^2x^2)}{(1-c_1c_2x)^2+4c_1c_2x\sin^2(\frac{\phi}{2})} \qquad \text{(Eq. 2.28)}$$

$$\frac{I_d}{I_i}(\phi) = \left|\frac{E_d}{E_i}\right|^2 = 1 - \frac{(1-c_1^2)\cdot(1-c_1^2)\cdot x}{(1-c_1c_2x)^2+4c_1c_2x\sin^2(\frac{\phi}{2})} \qquad \text{(Eq. 2.29)}$$

The transmission characteristic of the add/drop filter is given by Fig. 2.12

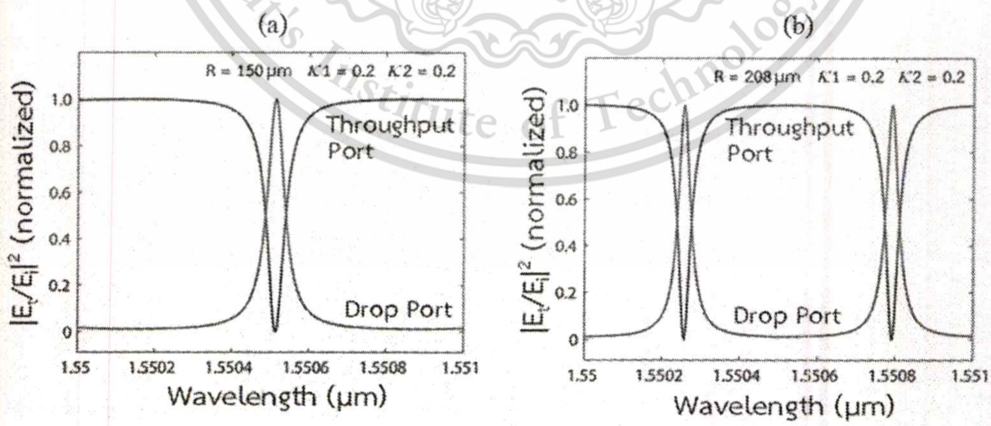

Fig. 2. 12 Transmission characteristic of add/drop filter where ring radius is varied

(a) $R = 150\,\mu m$, (b) $R = 208\,\mu m$

Where the coupling coefficients $K_1 = K_1 = 0.2$, and the ring radius of the add/drop device is varied to be (a) $R = 150\ \mu m$ and (b) $R = 208\ \mu m$. The outputs at the through port and the output at the drop port will be entirely out phase.

2.3.5 Interferences of Wave

Wave interference is the phenomenon that occurs when two waves meet while traveling along the same medium. The interference of waves causes the medium to take on a shape that results from the net effect of the two individual waves upon the particles of the medium. To begin our exploration of wave interference, consider two pulses of the same amplitude traveling in different directions along the same medium. Let's suppose that each displaced upward 1 unit at its crest and has the shape of a sine wave. As the sine pulses move towards each other, there will eventually be a moment in time when they are completely overlapped. At that moment, the resulting shape of the medium would be an upward displaced sine pulse with an amplitude of 2 units. The diagrams below depict the before and after interference snapshots of the medium for two such pulses.

When two waves are interfering, they can be either constructive or destructive interference. When two waves are same phase interference

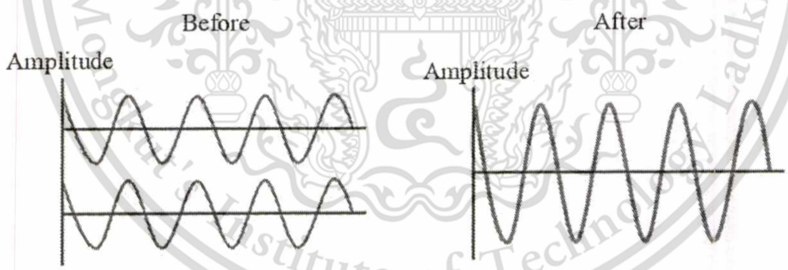

Fig. 2. 13 Show the constructive interference

This type of interference is sometimes called constructive interference. Constructive interference is a type of interference that occurs at any location along the medium where the two interfering waves have a displacement in the same direction. In this case, both waves have an upward displacement; consequently, the medium has an upward displacement that is greater than the displacement of the two interfering pulses. Constructive interference is observed at any location where the two interfering waves are displaced upward. But it is also observed when both interfering waves are displaced downward.

When two waves are different phase interference then the destructive interference is appeared. Destructive interference is a type of interference that occurs at any location along the medium where the two interfering waves have a displacement in the opposite direction. For instance, when a sine pulse with a maximum displacement of +1 unit meets a sine pulse with a maximum displacement of -1 unit, destructive interference occurs as shown in Fig. 2.14

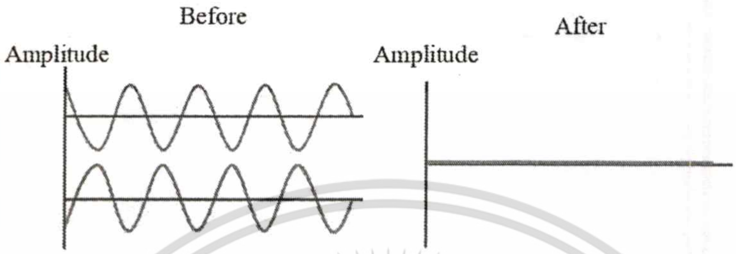

Fig. 2. 14 Show the destructive interference

In Fig. 2.14, the interfering pulses have the same maximum displacement but in opposite directions. The result is that the two pulses completely destroy each other when they are completely overlapped. At the instant of complete overlap, there is no resulting displacement of the particles of the medium. This "destruction" is not a permanent condition. In fact, to say that the two waves destroy each other can be partially misleading.

2.3.6 On-Off Resonance

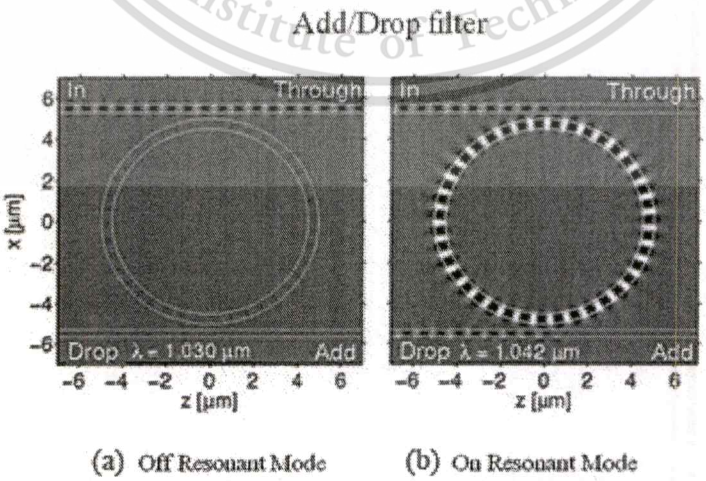

Fig. 2. 15 Show the resonance modes in add/drop filter

A resonant mode will have a wavelength that satisfies: $m\lambda_m = nL$, m is the longitudinal mode number, λ_m is the resonant mode wavelength n is the refractive index L is the circumference.

Off resonance: as shown in Fig. 2.15 (a) when a λ_1 wavelength propagated inside the ring N rounds and interfere with incomming wavelength λ_2 with the different phase (out phase), then the destructive interference is appeared in the ring, most power of light will be transmitted directly to the through port and only low power of light is transmitted to the drop port, this behavior is called as off-resonance mode.

On-resonance: as shown in Fig. 2.15 (b) when a λ_1 wavelength propagated in the ring N rounds and interfere with incomming wavelength with the same phase at λ_1 (in phase), then the constructive interference is appeared in the ring, most power of light will be transmitted directly to the drop port and only low power of light is transmitted to the through port, this behavior is called as on-resonance mode at λ_1.

2.4 Dark-Bright Soliton Conversion

In Fig. 2.16 shows the schematic of dark-bright solitons conversion system, where a stationary soliton pulse, which is introduced into the microring or a multi-stage microring resonator system, the input optical field (E_{in}) of the dark soliton pulse input is given by [24].

$$E_{in}(t) = A.tanh\left[\frac{T}{T_0}\right] exp\left[\left(\frac{z}{2L_D}\right) - i\omega_0 t\right] \quad \text{(Eq. 2.30)}$$

Where A is the optical field amplitude, z is the propagation distance, T is a soliton pulse propagation time in a frame moving at the group velocity, where ($T = t - \beta_1 z$), β_1 and β_2 are the coefficients of the linear and second-order terms of Taylor expansion of the propagation constant respectively, L_D is the dispersion length of the soliton pulse ($L_D = T_0^2/|\beta_2|$), T_0 is a soliton pulse propagation time of initial input (or soliton pulse width), t is the soliton phase shift time, ω_0 is the frequency shift of the soliton. This solution describes a pulse that keeps its temporal width invariance as it propagates, and thus is called a temporal soliton. When a soliton peak intensity ($\beta/\Gamma T_0^2$) is given, then T_0 is known. For the soliton pulse in the microring device, a balance should be achieved between the dispersion length (L_D) and the nonlinear length ($L_{NL} = 1/\Gamma\phi_{NL}$), where $\Gamma = n_2 k_0$ is the length scale over which dispersive or nonlinear effects make the beam become wider or narrower. For a soliton pulse, there is a balance between dispersion and nonlinear lengths, hence $L_D = L_{NL}$.

When light propagates within the nonlinear material (medium), the refractive index (n) of light within the medium is given by: $n = n_0 + n_2 I = n_0 + \left(\frac{n_2}{A_{eff}}\right) P$, where n_0 and n_2 are the linear and nonlinear refractive indexes, respectively. I and P are the optical intensity and optical power, respectively. The effective mode core area of the device is given by A_{eff}. For the microring and nanoring resonators, the effective mode core areas range from 0.50 to $0.1\ \mu m^2$ [25, 26].

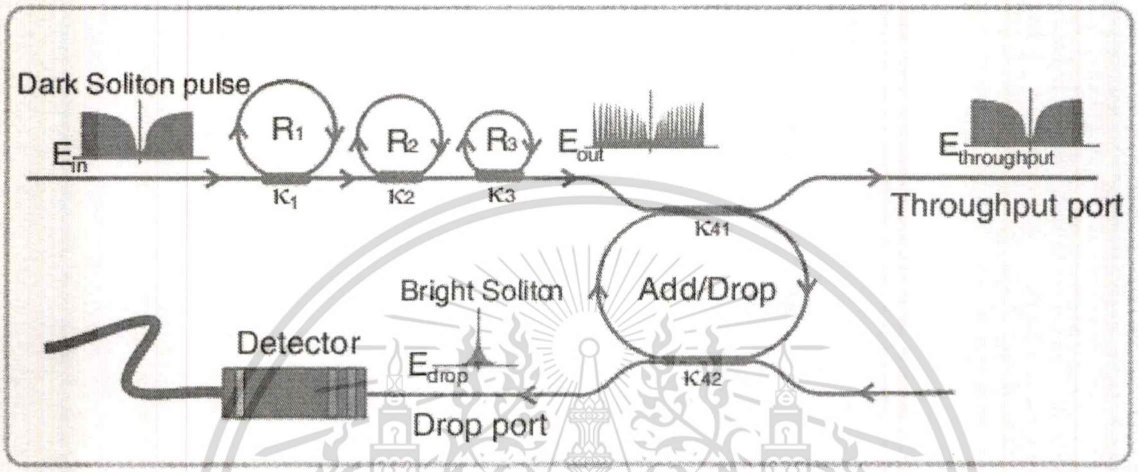

Fig. 2. 16 Schematic of dark-bright solitons conversion system

When a soliton pulse is input and propagated within a microring resonator as shown in Fig. 2.16, which consists of a series of microring resonators. The resonant output is formed, thus, the normalized output of the light field is the ratio between the output and input fields ($E_{out}(t)$ and $E_{in}(t)$) in each round-trip, which can be expressed as [27].

$$\left|\frac{E_{out}(t)}{E_{in}(t)}\right|^2 = (1-\gamma)\left[1 - \frac{(1-(1-\gamma)x^2)K}{(1-x\sqrt{1-\gamma}\sqrt{1-K})^2 + 4x\sqrt{1-\gamma}\sqrt{1-K}\sin^2\left(\frac{\emptyset}{2}\right)}\right] \quad \text{(Eq. 2.31)}$$

The close form of the Eq. 2.31 indicates that a ring resonator in this particular case is very similar to a Fabry-Perot cavity, which has an input and an output mirror with a field reflectivity, $(1-K)$, and a fully reflecting mirror. ·is the coupling coefficient, and $x = exp(-\alpha L/2)$ represents a round-trip loss coefficient, $\emptyset_0 = kLn_0$ and $\emptyset_{NL} = kLn_2|E_{in}|^2$ are the linear and nonlinear phase shifts, $k = 2\pi/\lambda$ is the wave propagation number in a vacuum where L and α are a waveguide length and linear absorption coefficient, respectively. In this work, the iterative method is introduced to obtain the results as shown in the Eq. 2.31 and similarly, when the output field is connected and input into the other ring resonators. After the signals are multiplexed with the generated chaotic noise, then the chaotic cancellation is required by the individual user. To retrieve the signals from the chaotic noise, we propose to use the add/drop device with the appropriate parameters. This is given in the details that follow. The optical circuits of ring-resonator add/drop filters for the throughput and drop port can be given by Eq. 2.32 and Eq. 2.33, respectively [28]

$$\left|\frac{E_t}{E_{in}}\right|^2 = \frac{(1-K_1)-2\sqrt{1-K_1}\cdot\sqrt{1-K_2}e^{-\frac{\alpha}{2}L}\cos(k_nL)+(1-K_2)e^{-\alpha L}}{1+(1-K_1)(1-K_2)e^{-\alpha L}-2\sqrt{1-K_1}\cdot\sqrt{1-K_2}e^{-\frac{\alpha}{2}L}\cos(k_nL)} \quad \text{(Eq. 2.32)}$$

And

$$\left|\frac{E_d}{E_{in}}\right|^2 = \frac{K_1K_2e^{-\frac{\alpha}{2}L}}{1+(1-K_1)(1-K_2)e^{-\alpha L}-2\sqrt{1-K_1}\cdot\sqrt{1-K_2}e^{-\frac{\alpha}{2}L}\cos(k_nL)} \quad \text{(Eq. 2.33)}$$

Where E_t and E_d represent the optical fields of the throughput and drop ports respectively. $\beta = kn_{eff}$ is the propagation constant, n_{eff} is the effective refractive index of the waveguide and the circumference of the ring is $L = 2\pi R$, here R is the radius of the ring. In the following, new parameters will be used for simplification: $\emptyset = \beta L$ is the phase constant. The chaotic noise cancellation can be managed by using the specific parameters of the add/drop device so that the required signals can be retrieved by the specific users. K_1 and K_2 are coupling coefficient of add/drop filters, $k_n = 2\pi/\lambda$, is the wave propagation number for a vacuum and the waveguide (ring resonator) loss is $\alpha = 0.5\ dBmm^{-1}$. The fractional coupler intensity loss is $\gamma = 0.1$. In the case of the add/drop device, the nonlinear refractive index is neglected.

In operation, a dark soliton pulse with $50\,ns$ pulse width, the maximum power of $0.65\,W$ is input into the dark-bright solitons conversion system as shown in Fig. 2.5. The suitable ring parameters are used, for instance, ring radii $R_1 = 10.0\ \mu m$, $R_2 = 7.0\ \mu m$, and $R_3 = 5.0\ \mu m$. In order to make the system compatible with the practical device, the selected parameters of the system are fixed to $\lambda_0 = 1.55\ \mu m\ 0$, $n_0 = 3.34$ (InGaAsP/InP). The light source used is the modulated Gaussian continuous wave. The effective core areas are $A_{eff} = 0.50, 0.25\ \mu m^2$ and $0.10\ \mu m^2$ for a microring and nanoring resonator [29], respectively. The waveguide loss and the coupling lose are $\alpha = 0.5\ dBmm^{-1}$, $\gamma = 0.1$, respectively, and the coupling coefficients (kappa, K) of the microring resonator range from 0.05 to 0.90. The nonlinear refractive index is $n_2 = 2.2 \times 10^{-13}\ m^2/W$. In this case, the wave guided loss used is $0.5\ dBmm^{-1}$. The input dark soliton pulse is sliced into the smaller signals as shown in Fig. 2.17 (a).

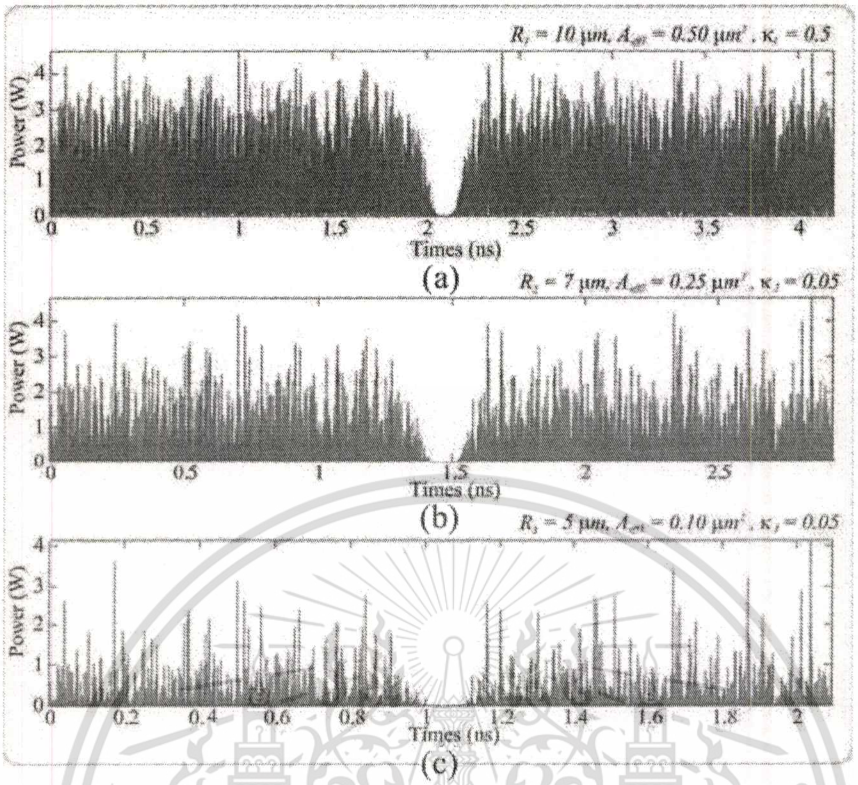

Fig. 2. 17 Simulation results of the soliton signals within the ring resonator system, where (a) in ring R_1, (b) in ring R_2, and (c) in ring R_3.

Figures 2.17 (b) and 2.17 (c) are the output signals of the filtering signals within the rings R_2 and R_3. They found that the output signals from R_3 are smaller than from R_1, which is more difficult to detect when it is used in the link. In fact, the multi-stage ring system is proposed due to the different core effective areas of the rings in the system, where the effective areas can be transferred from $0.50\ \mu m^2$ to $0.10\ \mu m^2$ with some losses. The soliton signals in R_3 are entered in the add/drop filter so the dark-bright solitons conversion can be performed by using Eq. 2.34 and Eq. 2.35. Results obtained when a dark soliton pulse is input into a micro and the nanoring resonator system are as shown in Fig. 2.18 and Fig. 2.19. The parameters used are the same as in Fig. 16, where the only change is the add/drop filter parameters. The add/drop filter is formed by two couplers and a ring radius (R_d) of $10\ \mu m$, the coupling constants (K_{11} and·K_{12}) are the same values (0.50). When the add/drop filter is connected to the third ring (R_3), the dark-bright solitons conversion is achieved and seen. The bright soliton and dark soliton are detected by the throughput and drop ports respectively

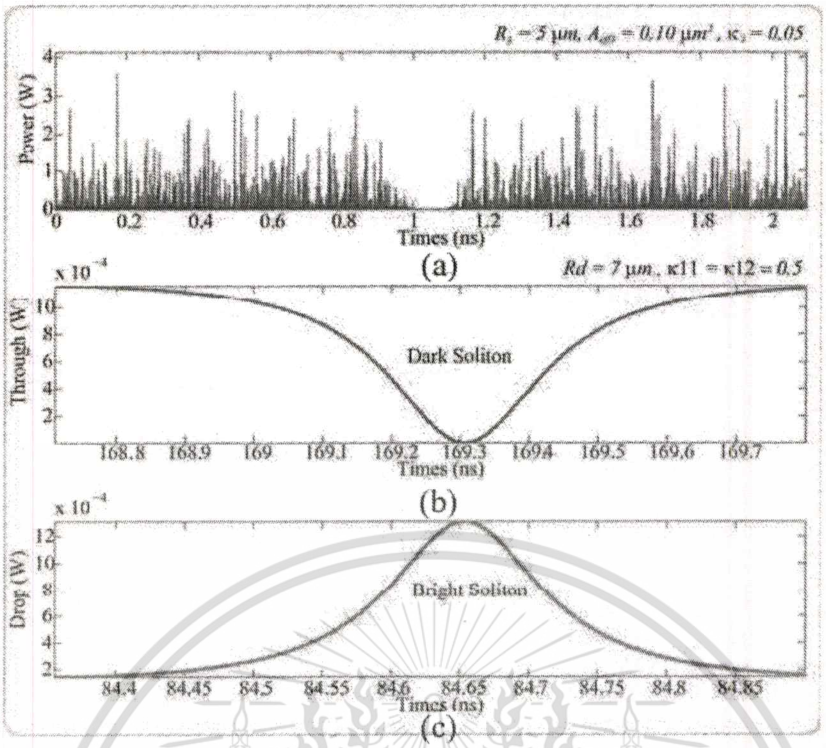

Fig. 2. 18 Simulation results of the optical solitons, where (a) the signals in R_3, (b) a dark soliton and (c) a bright soliton. The input dark soliton power is 0.65 W, $K_1 = 0.5$, $R_d = 10\,\mu m$.

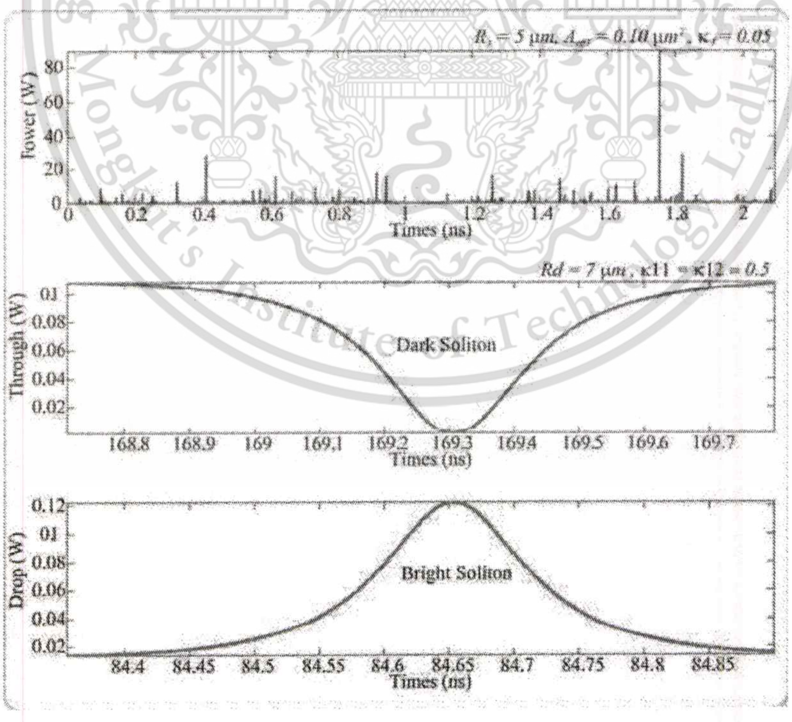

Fig. 2. 19 Simulation results of the optical solitons, where (a) the signals in R_3, (b) a dark soliton and (c) a bright soliton. The input dark soliton power is 0.65 W, $K_1 = 0.9$, $R_d = 10\,\mu m$.

Chapter 3

Design Optical Logic NAND Gate using Dark-Bright Soliton Conversion Control

3.1 Introduction

The optical logic gates are one of the key techniques in all-optical signal processing and communication network, in which the implementation of all-optical logic gates can be used in various methods for processing signals with light. Many researches have demonstrated various optical logic functions using different schemes. Therefore, the searching for new design has become the interesting work.

In this chapter proposes the one of the most important two logic gates namely NAND Gate based on dark-bright solitons conversions within the add/drop optical filter systems, which is a simple and flexible scheme for use as an arbitrary logic switching system. This can be used to form the advanced complex logic circuits, which will be detailed in the next section. For the concept of the optical logic NAND gate, the dark-bright solitons conversion in add/drop filters is the keyword of the system.

3.1.1 Dark-Bright Solitons Conversion Control in Add/Drop Filter

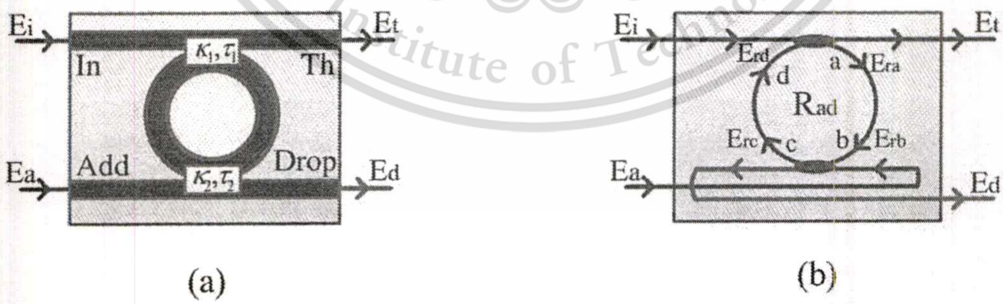

Fig. 3. 1 Schematic of an add/drop filter (AD)

In the operation of dark-bright solitons conversion system using an add/drop filter [25] as shown in Fig. 3.1, when for convenience, Fig. 3.1 (b) is replaced by Fig. 3.1 (a). The relative phase of the two output light signals after coupling into the optical coupler is $\pi/2$ before coupling into the ring and the input bus, respectively. This means that the signals coupled into the drop and through ports acquire a phase of π with respect to the input port signal. In application, if the coupling coefficients are formed appropriately, the field coupled into the throughput port would completely extinguish the resonant wavelength, and all power would be coupled into the drop port, in which the dark-bright conversion behaviors are described by Eq. 3.1 to Eq. 3.8, where we can consider the electric fields in each point from the equations below:

$$E_{ra} = -jk_1 E_i + \tau_1 E_{rd} \quad \text{(Eq. 3.1)}$$

$$E_{rb} = \exp(j\omega T/2)\exp(-\alpha L/4)E_{ra} \quad \text{(Eq. 3.2)}$$

$$E_{rc} = \tau_2 E_{rb} - jk_2 E_a \quad \text{(Eq. 3.3)}$$

$$E_{rd} = \exp(j\omega T/2)\exp(-\alpha L/4)E_{rc} \quad \text{(Eq. 3.4)}$$

$$E_t = \tau_1 E_i - jk_1 E_{rd} \quad \text{(Eq. 3.5)}$$

$$E_d = \tau_2 E_a - jk_2 E_{rb} \quad \text{(Eq. 3.6)}$$

Where E_i is the input field, E_a is the added (control) field, E_t is the throughput field, E_d is the dropped field, E_{ra} ... E_{rd} are the fields in the ring at points a ... d, K_1 is the field coupling coefficient between the input and the ring, K_2 is the field coupling coefficient between the ring and the output bus, L is the circumference of the ring ($2\pi R$), T is the time taken for one round trip ($T = Ln_{eff}/c$), and α is the power loss in the ring per unit length. We assume that lossless coupling (i.e. $\tau_{1,2} = \sqrt{1 - K_{1,2}^2}$). The output power-intensities at the drop port and the through port are given by π

$$|E_d|^2 = \left|\frac{-K_1 K_2 A_{1/2} \Phi_{1/2}}{1-\tau_1\tau_2 A\Phi} E_i + \frac{\tau_2 - \tau_1 A\Phi}{1-\tau_1\tau_2 A\Phi} E_a\right|^2 \quad \text{(Eq. 2.7)}$$

$$|E_t|^2 = \left|\frac{\tau_2 - \tau_1 A\Phi}{1-\tau_1\tau_2 A\Phi} E_i + \frac{-K_1 K_2 A_{1/2} \Phi_{1/2}}{1-\tau_1\tau_2 A\Phi} E_a\right|^2 \quad \text{(Eq. 2.8)}$$

Where $A_{1/2} = \exp(-\alpha L/4\,)$ is the half-round-trip amplitude ($A = A_{1/2}^2$),

$\Phi_{1/2} = \exp(j\omega T/2)$ is the half-round-trip phase contribution ($\Phi = \Phi_{1/2}^2$) .

The input optical field (E_i) and the add field (E_a) of dark soliton and bright are given by Eq. 2.4 and Eq. 2.5 as given in the previous chapter [8]

$$E_{in}(t) = A.tanh\left[\frac{T}{T_0}\right] exp\left[\left(\frac{z}{2L_D}\right) - i\omega_0 t\right] \quad \text{(Dark soliton)}$$

$$E_{in}(t) = A.sech\left[\frac{T}{T_0}\right] exp\left[\left(\frac{z}{2L_D}\right) - i\omega_0 t\right] \quad \text{(Bright soliton)}$$

Where A is the optical field amplitude, z is the propagation distance, T is a soliton pulse propagation time in a frame moving at the group velocity, where ($T = t - \beta_1 z$), β_1 and β_2 are the coefficients of the linear and second-order terms of Taylor expansion of the propagation constant respectively, L_D is the dispersion length of the soliton pulse ($L_D = T_0^2/|\beta_2|$), T_0 is a soliton pulse propagation time at initial input (or soliton pulse width), t is the soliton phase shift time, ω_0 is the frequency shift of the soliton.

3.2 Basic Block Diagram

In Fig 3.2 shows the schematic diagram of the designed system using for all-optical logic NAND gate, where A and B refer to the input logic signals represented by dark or bright soliton, T21 and D21 refer to the through port and drop port of add/drop filters No. 21, T22 and D22 refer to the through port and drop port of add/drop filters No. 22, respectively. The system consists of add/drop filters No. 01, No. 11, No. 21 and No. 22 respectively.

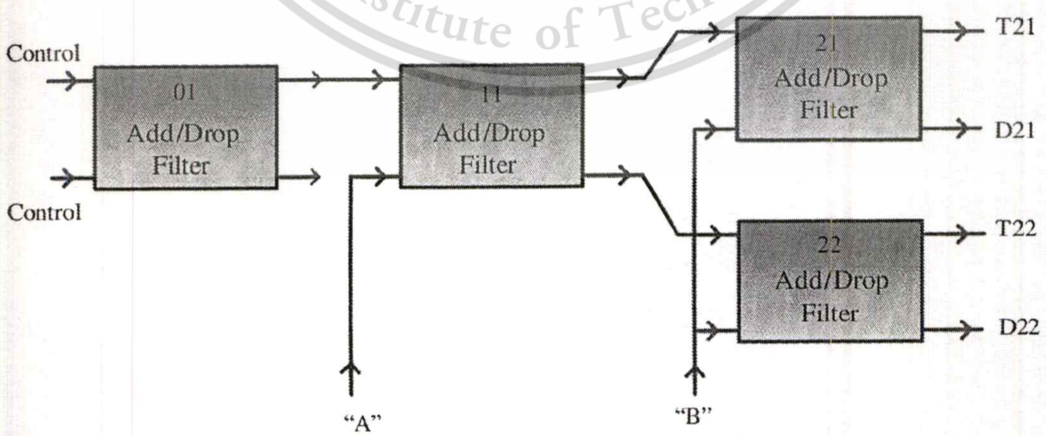

Fig. 3. 2 Schematic diagram of the proposed optical logic NAND gate system

First of all, the input and control light pulse trains are input in to the first add/drop optical filter (*No. 01*) using the dark-bright soliton where firstly, the dark soliton is converted to be dark and bright solitons via the add/drop optical filter (No. 01), which can be seen at through and drop ports with π phase shift, respectively.

By using add/drop filter (No.11), the input signal is generated by the first stage of add/drop optical filter (No. 01). Next, the input data A with logic "0" (dark soliton) and logic "1" (bright soliton) are added into the add port of add/drop filter No. 11. Secondly, the dark-bright solitons conversion with π phase shift is operated again.

Finally, by using add/drop filters (No. 21 and No. 22), both input signals are generated by the second stage of add/drop optical filter (*No. 11*), the input data B with logic "0" (dark soliton) and logic "1" (bright soliton) are added into the add ports of add/drop filters (No. 21 and No. 22). For large scale (see Fig. 3.2), the obtained results are simultaneously seen at the through and drop ports of add/drop filters *No. 21* and *No. 22* at T21, D21, D22, T22, where T21 is used for optical logic NAND gate and D21 and T22 is used for buffer gates A and B, respectively.

3.3 Simulation Results

In the simulation of the optical logic NAND gate, the used parameters of the add/drop filters are fixed as shown in Table 3.1. The result of the all-optical logic NAND gate is generated by using dark-bright solitons conversion with wavelength center at $\lambda_0 = 1.50\ \mu m$ which is widely used in the optical communication, pulse width is $35\ fs$, and input data logic "0" is formed by dark soliton pulse and logic "1" is formed by bright soliton pulse respectively.

Table 3. 1 The used parameters of dark-bright soliton inputs for optical logic NAND gate

Parameters of all input signals dark-bright solitons	Value
Signal power: P	$1\ \mu W$
Center wavelength: λ_0	$1.50\ \mu m$
Pulse width	$35\ fs$

Table 3. 2 The used parameters of all optical add/drop filters for optical logic NAND gate

Parameters of all add/drop filters	Value
Materials type	$\boldsymbol{GaAsP/InP}$
All coupling coefficients: K_s	0.05
Ring radius of all add/drop filters: R_{ad}	1.51 μm
Effective mode core area: A_{eff}	0.25 μm^2
Ring resonator attenuation coefficient loss: α	0.05 $dBmm^{-1}$
Fractional coupling intensity loss: γ	0.01
Effective refractive index: n_{eff}	3.14

When the input data logic "00" (DD) is added, the obtained output optical logic is "1000" (BDDD), as shown at the through and drop ports T21, D21, T22 and D22, respectively see [Fig. 3.3]

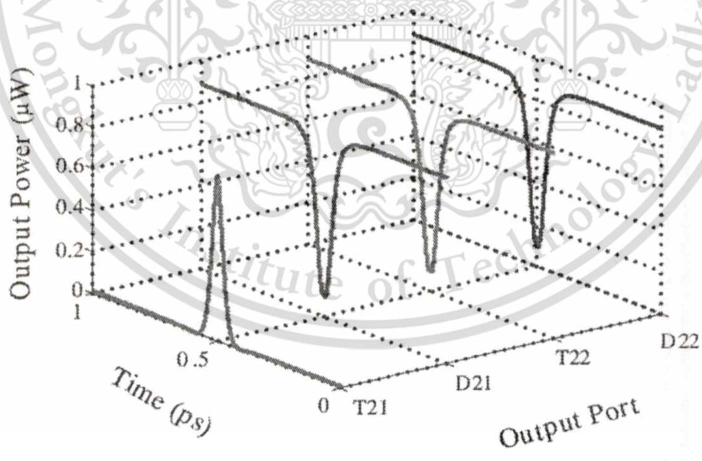

Fig. 3. 3 Show the output logic when the input stages '00' or 'DD'

When the input data logic "01" (DB) is added, the output optical logic "1010" (BDBD) is obtained, see [Fig. 3.4]

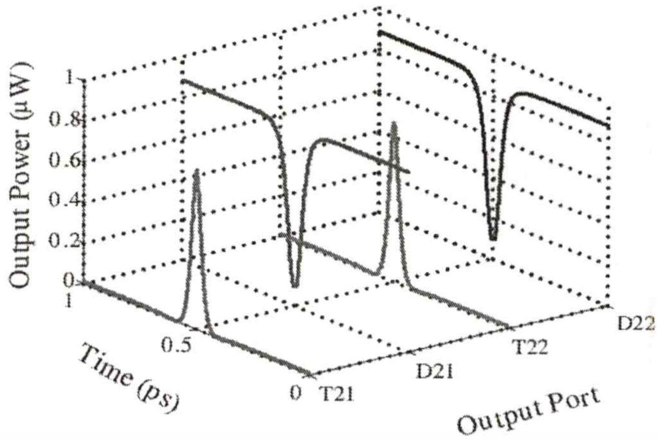

Fig. 3. 4 Show the output logic when the input stages '01' or 'DB'

When the input data logic "10" (BD) is added, the output optical logic "1100" (BBDD) is obtained, see [Fig. 3.5]

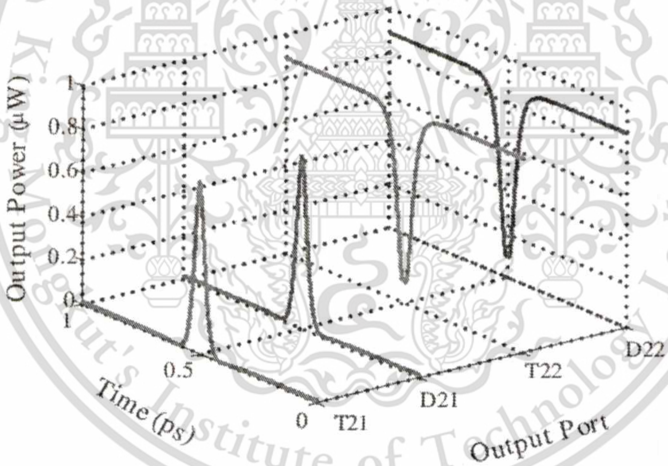

Fig. 3. 5 Show the output logic when the input stages '10' or 'BD'

Finally, when the input data logic "11" (BB) is added, we found that the output optical logic "0110" (DBBD) is obtained, see [Fig. 3.6]

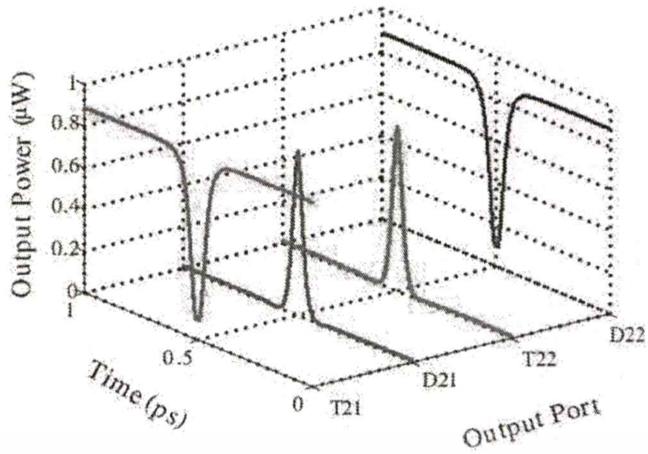

Fig. 3. 6 Show the output logic when the input stages '11' or 'BB'

Table 3. 3 Conclusion of Truth Table NAND Gate

Input A 0 (D), 1 (B)	Input B 0 (D), 1 (B)	Output T21 0 (D), 1 (B)	Output D21 0 (D), 1 (B)	Output T22 0 (D), 1 (B)	Output D22 0 (D), 1 (B)
0	0	1	0	0	**0**
0	1	1	0	1	**0**
1	0	1	1	0	**0**
1	1	0	1	1	**0**

3.3.1 Discussion

In the simulation result of the optical logic NAND gate shows that the dark-bright soliton conversion concept is can be performed by logic 1 is bright soliton, and logic 0 is dark soliton, with center wavelength at $\lambda_0 = 1.50\ \mu m$ in the add/drop filter where the AD ring resonator is $R_{ad} = 1.51\ \mu m$, however we can still use other value of ring radius, the discussion and the experimental results of changing add/drop parameters will be demonstrated in the next chapter, i.e. optical S-R flip-flop using dark-bright solitons conversion control. In the concept of optical S-R flip-flop is used the same techniques with the optical logic gates so the discussion will be skipped in this section.

3.4 Summary

We found that output data logic at the through port T21 is optical logic NAND Gate, the output data logic at drop port D21 and through port T22 are same with the input A and B respectively. We have shown that the proposed photonic circuit can be used to create the logic NAND Gate. With the input data logic "0" (dark soliton) and logic "1" (bright soliton), the all-optical device can perform the optical logic NAND at the T21 output. This could be a potential key component in the all-optical signal processing, which is a simple and flexible scheme that can be used to perform the advanced logic switching system. This can be extended and implemented for any higher number of input digits by the proper incorporation of dark-bright soliton conversion control, based optical switches.

The used parameters are fixed to be all coupling coefficients to be $K_s = 0.05$, $R_{ad} = 1.51\ \mu m$, $A_{eff} = 0.25\ \mu m^2$, $a = 0.05\ dBmm^{-1}$, $\gamma = 0.01$, $n_{eff} = 3.14$ (for ***GaAsP/InP***) for all add/drop optical filters in the system. The result of the all-optical NAND gate is generated by using dark-bright soliton conversion with wavelength center at $\lambda_0 = 1.50\ \mu m$, pulse width 35 *fs* and input data logic "0" (D) and logic "1" (B). When the input data logic "00" is added, the obtained output optical logic is "1000". When the input data logic "01" is added, the output optical logic "1010" is obtained. When the input data logic "10" is added, the output optical logic "1100" is obtained. When the input data logic "11" is added, we found that the output optical logic "0110" is seen at through and drop ports T21, D21, T22, D22 respectively. The outputs can be used to perform the optical logic NAND gate at through port T21.

Chapter 4

Design Optical S-R Flip-Flop using Dark-Bright Soliton Conversion Control

4.1 Introduction

Nowadays, All-optical flip-flop has become an essential component of latching functions in ultra high speed all-optical processing applications [15, 16]. Many systems for performing optical flip-flops using different optical techniques have been proposed. An optical flip-flop is the packet switches in the next generation of communication network. The flip-flop is a logic gate that maintains a stable state output even after the input is turned off, in which the key basic function is represented by the logic gates (NOR, NAND).

S-R flip-flop is a circuit with two cross-coupled NOR gates or two cross-coupled NAND gates. It has two input signals, which one is S and the other is R for setting and resetting the outputs Q_{n+1} and $\overline{Q}_{n+1}$ respectively. The S-R flip-flop outputs are the feedback signals. There are three statuses of logic output signals, which is called "Hold" state when no input signal (S = 0, R = 0), it is called "Set" state when input signals are (S = 1, R = 0), and it is called "Reset" state when input signals are (S = 0, R = 1) respectively. For in case of (S = 1, R = 1) is not allowed, or we can call "Forbidden" state.

In this chapter, we have presented an optical S-R flip-flop system using dark-bright soliton conversion control. For our concept, the optical S-R flip-flop operation of binary based on dark-bright solitons conversion behaviors can be performed, in which the coincidence dark and bright soliton pulses can be separated after propagating into the optical-filter device with $\pi/2$ phase shifted (an optical coupler) [18]. The proposed scheme is based on a 1 bit binary to the complex logic circuits, which can be compared by any 2 bits, when logic '0' and '1' are formed by dark and bright soliton pulses, respectively.

4.2 Basic Block Diagram

Based on the applications of logic gates using dark-bright solitons conversion control techniques as demonstrated in the previous chapter. We have designed a schematic for an optical S-R flip-flop for higher speed and flexible memory or signal processing applications, the schematic for optical S-R flip-flop using dark-bright soliton conversion control (see Fig. 4.1).

In Fig 4.1 shows the schematic diagram of the designed system using for all-optical S-R flip-flop, where S and R refer to the input signals represented by dark or bright soliton respectively, Q_{n+1} and $\overline{Q}_{n+1}$ refer to the outputs of the optical S-R flip-flop circuit represented by dark or bright soliton respectively, AD1 and AD2 refer to the add/drop filters No. 1 and No. 2, respectively.

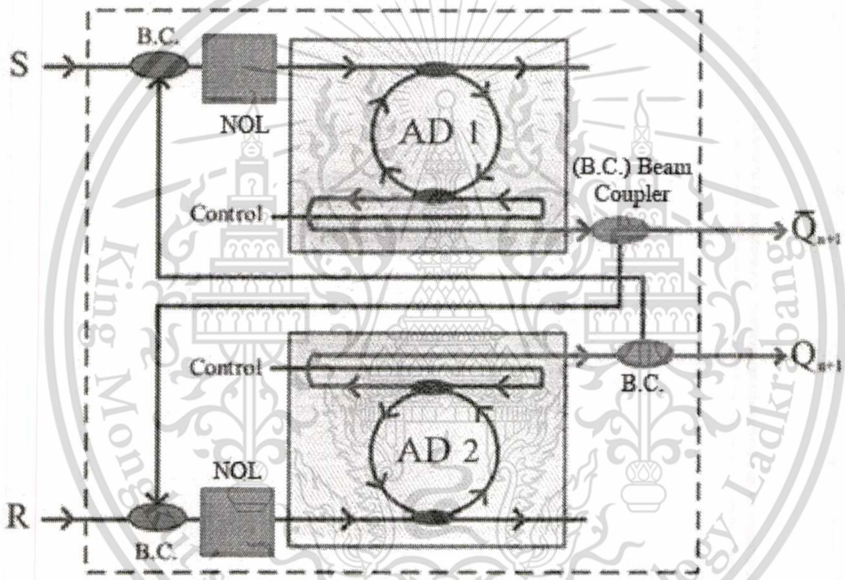

Fig. 4. 1 Schematic diagram of the design optical S-R flip-flop

The proposed scheme has two optical add/drop filters (AD1 and AD2) integrated with four beam coupler (B.C.), and two nonlinear optical amplifier (NOL), where firstly, the input logic '1' is formed by bright soliton (B) and logic '0' is formed by the absence of the input signal. The other technique that can be used to form the similar operation can be found in reference [54], in which the optical power signal is manipulated by NOL. NOL is used to control the feedback input power, a beam coupler is used to split the output light into two waves that travel in opposite directions and acquire different phases because of nonlinearities in the optical medium; the output power is very low for some phase differences and combine two beams by reversing the direction of the light from two outputs to two inputs.

NOL can be either micro ring resonator or EDFA [56] or nolinear ring resonator [57, 58], if we use the Erbium-Doped Fiber Amplifier (EDFA) to manipulated the signal the system need to be in a bigger size system design, or using the nonlinear ring resonator, the system can be design in a smaller size device.

4.3 Optical S-R Flip-Flop Circuit

Case 1: When it is no input signal, S = R = 0, where Q_{n+1} and $\overline{Q}_{n+1}$ are not changed. This state is called "Hold"

Case 2: By using the dark-bright solitons conversion behavior, when S = 0, R = 1, the input logic '0' and '1' are formed by dark-bright solitons, where both input signals are converted to dark-bright solitons pulses with π phase shift. The add/drop filter AD1 receives the logic '0' (dark soliton), i.e. $Q_{n+1} = 0$, which is connected to the input 'S', then the dark-bright solitons conversion with π phase shift is operated again. When the add/drop filter AD2 receives the logic '1' (bright soliton), hence $Q_{n+1} = 1$ [see Fig. 4.2], in which Q_{n+1} and $\overline{Q}_{n+1}$ are connected to the input 'S' and 'R', respectively. Therefore, if both 'S' and 'R' are no input signals, i.e. S = R = 0. Then Q_{n+1} and $\overline{Q}_{n+1}$ are the feedback signals, which is called the "Reset".

Case 3: When S = 1 and R = 0, the logic '0' and '1' are formed by dark-bright soliton, where both input signals are converted to dark -bright solitons with π phase shift. When AD1 receives the logic '0' (dark soliton) i.e. $\overline{Q}_{n+1} = 0$, which is connected to the input 'R', then the dark-bright solitons conversion with π phase shift is formed. When the AD2 receives the logic '1' (bright soliton), hence $Q_{n+1} = 1$ [see Fig. 4.3], where Q_{n+1} and $\overline{Q}_{n+1}$ are connected to the input 'S' and 'R', respectively. Therefore, if both 'S' and 'R' are no input signals, i.e. S = R = 0. Then Q_{n+1} and $\overline{Q}_{n+1}$ are the feedback signals, which is called the "Set".

Case 4: When S = R = 1 then both AD1 and AD2 receive both the incoming bright soliton signals, i.e. $Q_{n+1} = \overline{Q}_{n+1} = 1$, this state is called the "Forbidden" see Fig. 4.4.

4.4 Simulation Results

In the simulation of the optical S-R flip-flop, the used parameters of the add/drop filters are fixed as shown in Table 4.1. The results of the optical flip-flop are generated by using dark-bright solitons conversion with wavelength center at $\lambda_0 = 1.50\,\mu m$ which is widely used in the optical communication, soliton pulse width is 35 fs, (see Table 4.2), and input data logic "0" is formed by dark soliton pulse and logic "1" is formed by bright soliton pulse respectively.

Table 4. 1 The used parameters of all optical add/drop filters for optical S-R flip-flop

Parameters of all add/drop filters	Value
Materials type	$GaAsP/InP$
All coupling coefficients: K_s	0.5
Ring radius of all add/drop filters: R_{ad}	1.55 μm
Effective mode core area: A_{eff}	0.25 μm^2
Ring resonator attenuation coefficient loss: α	0.05 $dBmm^{-1}$
Fractional coupling intensity loss: γ	0.01
Effective refractive index: n_{eff}	3.14

Table 4. 2 The used parameters of dark-brightsolitons inputs for optical S-R flip-flop

Parameters of all input signals dark-bright solitons	Value
Signal power: P	1 μW
Center wavelength: λ_0	1.50 μm
Soliton pulse width	35 fs

In the simulation results, the output power is already manipulated by EDFA, after the inputs S = 0 (D) and R=1 (B) are input into the system then we can obtain the outputs at through and drop ports T1 = 0 (D), D1 = 1 (B), D2 = 0 (D), and T2 = 1 (B), respectively (see Fig. 4.2), the output Q_{n+1} is seen at drop port D1, and the output Q_{n+1} is seen at drop port D2

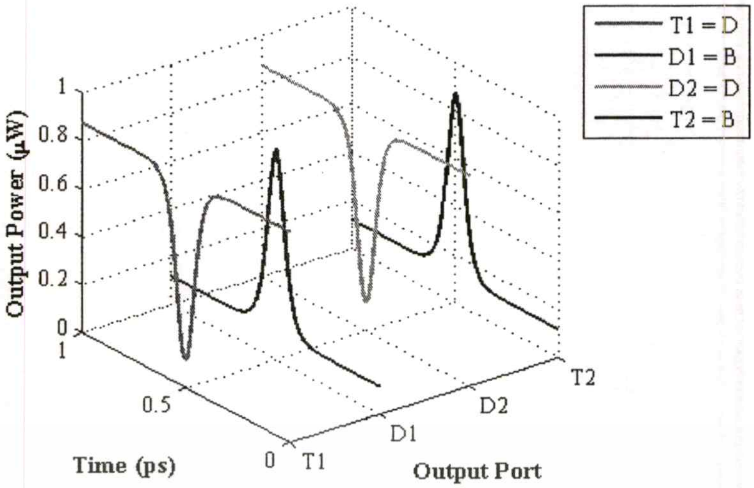

Fig. 4. 2 Show the outputs when "Reset" state

After the inputs S = 1 (B) and R=0 (D) are input into the system then we can obtain the outputs at through and drop ports T1 = 1 (B), D1 = 0 (D), D2 = 1 (B), and T2 = 0 (D), respectively (see Fig. 4.3)

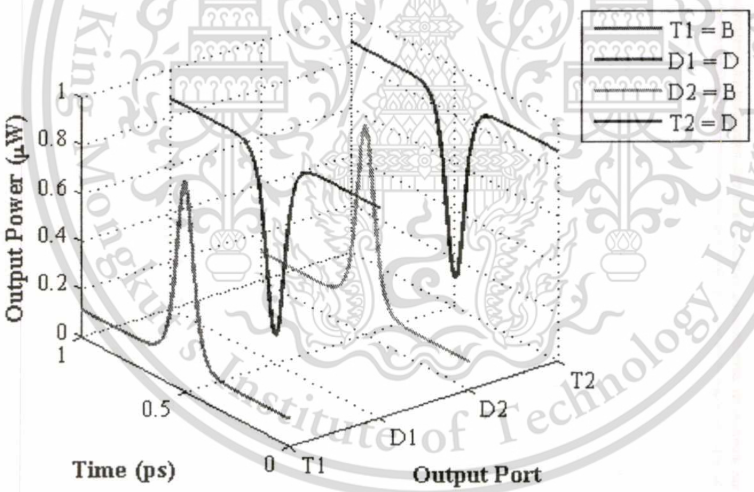

Fig. 4. 3 Show the outputs when "Set" state

After the inputs S = 1 (B) and R=1 (B) are input into the system then we can obtain the outputs at through and drop ports T1 = 0 (D), D1 = 1 (B), D2 = 1 (B), and T2 = 0 (D), respectively (see Fig. 4.4)

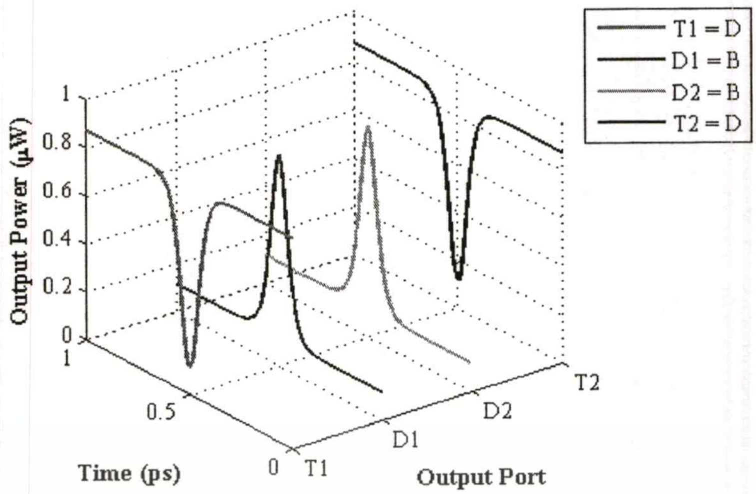

Fig. 4. 4 Show the outputs when "Forbidden" state

Table 4. 3 Conclusion of truth table for optical S-R flip-flop

Inputs (D = 0, B = 1)		**Outputs** (D = 0, B = 1)		**States**
S	**R**	$\mathbf{Q_{n+1}}$ **(D1)**	$\mathbf{\overline{Q}_{n+1}}$ **(D2)**	
D	D	$\mathbf{Q_{n+1}}$	$\mathbf{\overline{Q}_{n+1}}$	Hold
D	B	D	B	Reset
B	D	B	D	Set
B	B	B	B	Forbidden

4.4.1 Experiment of Changing the AD Ring Radius

In our proposed system is designed for the optical S-R flip-flop that obtains the stable output power, the used of all AD ring radius are $R_{ad} = 1.55\ \mu m$, for the simulation as mentioned in the previous section. However, it is possible to use the AD ring resonator bigger or smaller than $1.55\ \mu m$ in some values as well in some specific system. In this experiment we used two tests (test 1 and test 2) as shown in Fig. 4.5 and Fig. 4.6, respectively, the used parameters of the simulation Test 1 and Test 2 are shown in Table 4.4, and the input power is all the same.

Table 4. 4 The used parameters of all AD filters for the experiment (Test 1 and Test 2)

Parameters of all add/drop filters	Original values	Test 1 values	Test 2 values
Materials type	$InGaAsP/InP$	$InGaAsP/InP$	$InGaAsP/InP$
All coupling coefficients: K_s	0.5	0.5	0.5
Ring radius of all add/drop filters: R_{ad}	1.55 μm	(a) 1.53 μm (b) 1.525 μm	(a) 1.58 μm (b) 1.59 μm
Effective mode core area: A_{eff}	0.25 μm^2	0.25 μm^2	0.25 μm^2
Attenuation coefficient loss: α	0.05 $dBmm^{-1}$	0.05 $dBmm^{-1}$	0.05 $dBmm^{-1}$
Fractional coupling intensity loss: γ	0.01	0.01	0.01
Effective refractive index: n_{eff}	3.14	3.14	3.14

Test 1 uses the AD ring radius $R_{ad} = 1.53\ \mu m, 1.525\ \mu m,$ respectively. This simulation results are demonstrated that our proposed system affects to the output power by the change of the AD ring radius to be smaller, it affects to the output power to become smaller too as shown in Fig. 4.5, and the change of output at through and drop ports as shown in Fig. 4.5, however it can still obtain the output logic for optical S-R flip-flop in some values of AD ring radius.

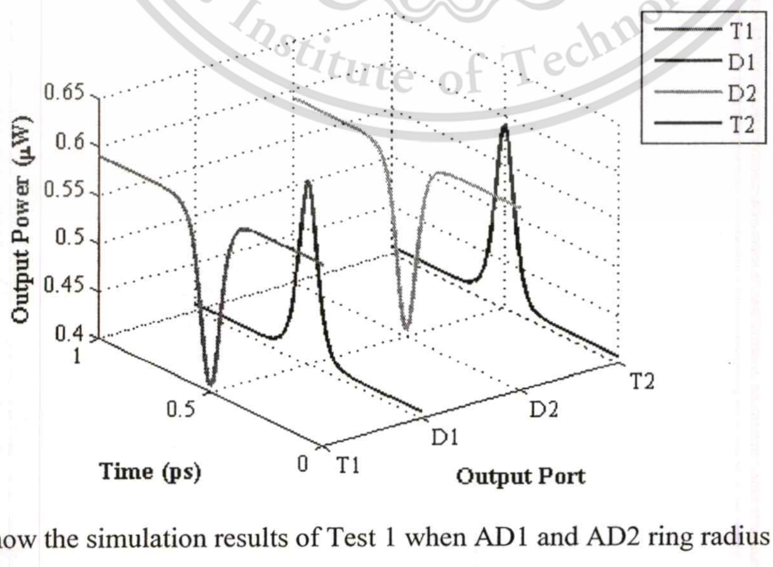

Fig. 4. 5 Show the simulation results of Test 1 when AD1 and AD2 ring radius $R_{ad} = 1.53\ \mu m$, inputs S = 0 (D) and R = 1 (B)

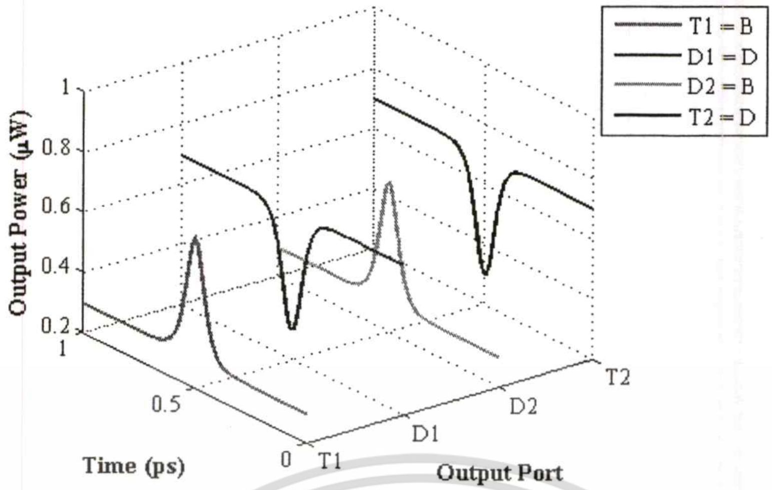

Fig. 4. 6 Show the simulation results of Test 1 when AD1 and AD2 ring radius $R_{ad} = 1.525\,\mu m$, inputs S = 0 (D) and R = 1 (B)

Test 2 uses the AD ring radius $R_{ad} = 1.58\,\mu m, 1.59\,\mu m$, respectively. This simulation results are demonstrated that our proposed system affects to the output power by the change of the AD ring radius to become bigger, some values of the AD ring radius affect the change of output power and output at through and drop ports as shown in Fig. 4.7 and Fig. 4.8

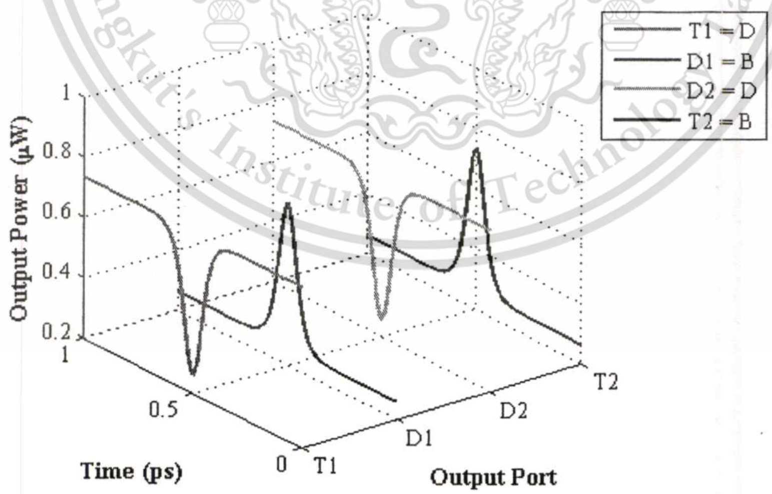

Fig. 4. 7 Show the simulation outputs of Test 2 when AD1 and AD2 ring radius $R_{ad} = 1.58\,\mu m$, inputs S = 0 (D) and R = 1 (B)

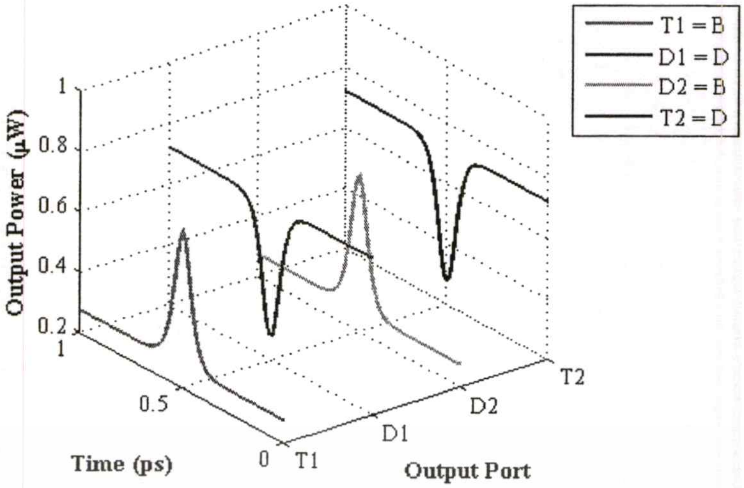

Fig. 4. 8 Show the simulation outputs of Test 2 when AD1 and AD2 ring radius $R_{ad} = 1.59\,\mu m$, inputs S = 0 (D) and R = 1 (B)

Table 4. 5 Conclusion of output power when all parameters are fixed, and the ring radius is changed

AD ring radius	Output power (μm)				S-R flip-flop
R_{ad} (μm)	T1	D1 ($\overline{\mathbf{Q}}_{\mathbf{n+1}}$)	D2 ($\mathbf{Q}_{\mathbf{n+1}}$)	T2	When S = 0, R = 1
1.25	0.11	0.89	0.11	0.89	yes
1.30	0.511	0.489	0.511	0.489	no
1.35	0.22	0.68	0.22	0.68	yes
1.40	0.11	0.89	0.11	0.89	yes
1.45	0.64	0.36	0.64	0.36	no
1.50	0.20	0.80	0.20	0.80	yes
1.55	0.12	0.88	0.12	0.88	yes
1.60	0.77	0.23	0.77	0.23	no
0.35	0.12	0.88	0.12	0.88	yes
0.5	0.11	0.89	0.11	0.89	yes
0.65	0.11	0.89	0.11	0.89	yes
1.85	0.13	0.87	0.13	0.87	yes
2.00	0.14	0.86	0.14	0.86	yes
2.15	0.15	0.85	0.15	0.85	yes

In Table 4.5 shows the outputs when the ring radius is varied, all parameters are fixed to be $K_s = 0.5$, $A_{eff} = 0.25\ \mu m^2$, $\alpha = 0.05\ dBmm^{-1}$, $\gamma = 0.01$, $n_{eff} = 3.14$, by using dark-bright soliton with wavelength center at $\lambda_0 = 1.50\ \mu m$, pulse width $35\ fs$.

The outputs show that the AD ring radius can be smaller or bigger than $R_{ad} = 1.55\ \mu m$, and the effective values of AD ring radius are $R_{min} \leq (R_{ad}: R_{ad} - 0.15: R_{min})\ \mu m$, i.e. $1.40\ \mu m$, $1.25\ \mu m$, ... $0.35\ \mu m$, where the other parameters are not changed, and $R_{max} \geq (R_{ad}: R_{ad} + 0.15: R_{max})\ \mu m$, i.e. $1.70\ \mu m$, , $1.85\ \mu m$, $2.00\ \mu m$.

4.4.2 Experiment of Changing the AD Coupling Coefficients

In our proposed system is designed for the optical S-R flip-flop that obtains the stable output power, the used of all AD coupling coefficient are $K_s = 0.5$, for the simulation as mentioned in the previous section. However, it is might possible to use the AD coupling coefficient in other values as well in some specific system. In this experiment we used two tests (two values of coupling coefficients) as shown in Fig. 4.9 and Fig. 4.10, respectively, the used parameters of the simulation Test are shown in Table 4.5, and the input power is all the same

Table 4. 6 The used parameters of all AD filters for the experiment (Test 1)

Parameters of all add/drop filters	Original values	Test values
Materials type	$InGaAsP/InP$	$InGaAsP/InP$
All coupling coefficients: K_s	0.5	(a) 0.1 (b) 0.8
Ring radius of all add/drop filters: R_{ad}	$1.55\ \mu m$	$1.55\ \mu m$
Effective mode core area: A_{eff}	$0.25\ \mu m^2$	$0.25\ \mu m^2$
Attenuation coefficient loss: α	$0.05\ dBmm^{-1}$	$0.05\ dBmm^{-1}$
Fractional coupling intensity loss: γ	0.01	0.01
Effective refractive index: n_{eff}	3.14	3.14

In Test uses the AD coupling coefficient are $K_S = 0.1, 0.8$ respectively. This simulation results are demonstrated that our proposed system affects to the output power by the change of the AD coupling coefficient to be smaller or bigger, it affects to the output power to become smaller or bigger at through and drop ports as shown in Fig. 4.9 and Fig. 4.10, however it can still obtain the output logic for optical S-R flip-flop in some values of AD coupling coefficients

The simulation results after when the AD coupling coefficients are changed:

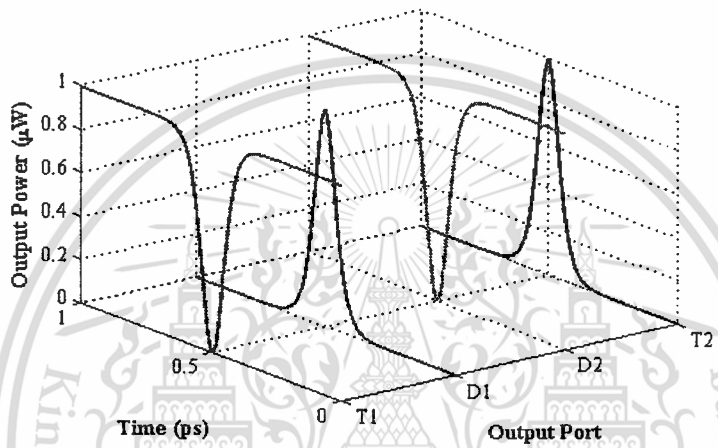

Fig. 4. 9 Show the simulation outputs of the Test when AD1 and AD2 all coupling coefficients is $K_S = 0.1$, inputs S = 0 (D) and R = 1 (B)

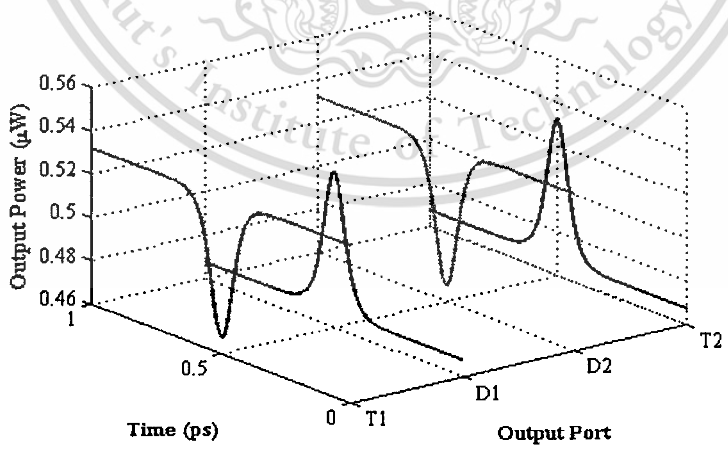

Fig. 4. 10 Show the simulation outputs of the Test when AD1 and AD2 all coupling coefficients is $K_S = 0.8$, inputs S = 0 (D) and R = 1 (B)

4.4.3 Experiment of Changing the Inputs Power

In our proposed system uses for the optical soliton input power is $1\,\mu W$, the used of all AD ring radius are $R_{ad} = 1.55\,\mu m$, for the simulation as mentioned in the previous section. However, it is possible to use input power in $1\,mW$ as well in some specific system. In this experiment we used two tests (test 1 and test 2) as shown in Fig. 4.11 and Fig. 4.12, respectively, the used parameters of AD in the simulation Test 1 and Test 2 are shown in Table 4.1 [at the previous section], and the input power is shown in table 4.7.

Table 4. 7 The used parameters of dark-bright soliton input power for Test 1 and Test 2

Parameters of all input signals of dark-bright solitons	Original value	Value of test 1	Value of test 2
Signal power: P	$1\,\mu W$	$1.5\,mW$	$1\,mW$
Center wavelength: λ_0	$1.50\,\mu m$	$1.50\,\mu m$	$1.50\,\mu m$
Soliton pulse width	$35\,fs$	$35\,fs$	$35\,fs$

The simulation results after the input power is changed to be $1.5\,mW$ and the parameters are not changed.

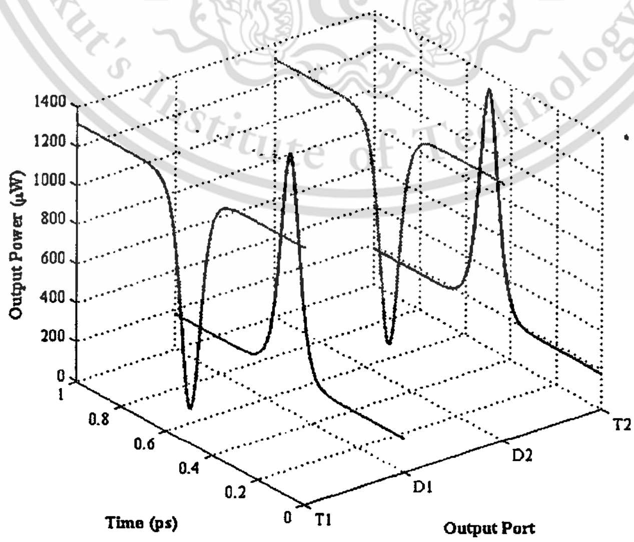

Fig. 4. 11 Show the simulation outputs of the Test 1 when input power is 1.5 mW, inputs S = 0 (D) and R = 1 (B)

The simulation results after the input power is changed to be 1 mW

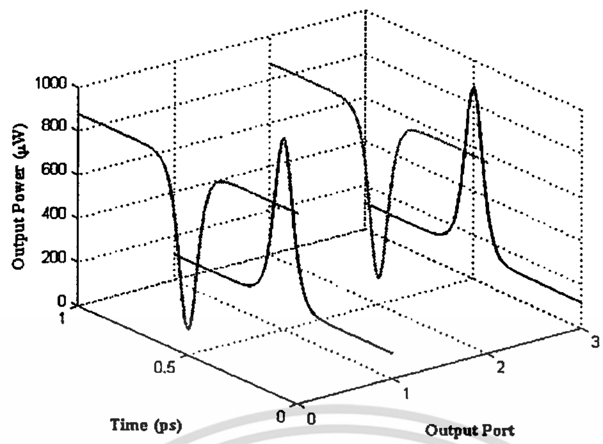

Fig. 4. 12 Show the simulation outputs of the Test 2 when input power is 1 mW, inputs S = 0 (D) and R = 1 (B)

4.5 Discussion

In the simulation results as shown in the previous section is demonstrated that the change of the AD ring resonator radius is affected to the output phases at through ports, some values of ring radius obtains the output logic 1 at through port and logic 0 at drop port when input logic 1 is added at the input port and logic 0 is added at the add port, but some value of radius obtains the output logic 0 at through port and logic 1 at drop port when the same input. The coupling coefficients also affect to the output power of through and drop ports, when the coupling coefficients are increased then the output power are decreased, in another way, when the coupling coefficients are decreased then the output power are increased.

In Fig. 4.5 shows that when the AD ring resonator is changed, where dark soliton is input into the input port and coupled into the ring and bright soliton is added into the add port, where in Fig. 4.5 is the off resonant mode, where the dark soliton is appeared at through port T1, simultaneously when the bright soliton is appeared at drop port D1. In Fig. 4.6 where dark soliton is input into the input port and coupled into the ring bright soliton is added into the add port is the on resonant mode, where the bright soliton is appeared at through port T1, simultaneously the drk soliton is appeared at drop port D1. In Fig. 4.7 and Fig. 4.8 are the same case.

In Fig. 4.9 shows that when the coupling coefficients K_S are changed, where in Fig. 4.9, K_S become smaller, then the obtained output power at through and drop ports are increased, in Fig. 4.10,

$K_s = 0.8$, then the obtained output power at through and drop ports are decreased. We can said that the add/drop ring radius and coupling coefficient are affect to the output pwer at through and drop ports, when all parameters are not change.

In Fig. 4.11 and Fig. 4.12 show that when the out put power are changed, where all parameters are not change, the output power is depend on the coupling loss and the attenuation loss of the ring.

4.6 Summary

We proposed new designed for basic all-optical flip-flop operations based on dark-br ight solitons conversion control system via the modified add/drop filters for ultrahigh speed memory or signal processing application. Based on the dark-bright solitons conversion control concept, the data logic '0' (dark soliton) and '1' (bright soliton) using all-optical in nature can be used to form the flip-flop operations, in which the logic status results can be obtained simultaneously at the drop and through ports, respectively. Therefore, the proposed design can be used for logical circuit which is recognized as the simple and flexible system for performing the logic switching system. Moreover, such device can be extended and implemented for any flip-flop such as S-R, D, T and J-K flip-flop by a proper incorporation of dark-bright solitons conversion control based optical switches, which can be available for more advanced applications.

The used parameters are fixed to be all coupling coefficients to be $K_s = 0.1 - 0.5$, all AD ring radius $R_{ad} = 1.55\,\mu m$, the effective mode core area $A_{eff} = 0.25\,\mu m^2$, waveguide attenuation loss $a = 0.05\,dBmm^{-1}$, coupling loss $\gamma = 0.01$, refractive index $n_{eff} = 3.14$ (for ***GaAsP/InP***) for all AD in the system. Result of the optical S-R flip-flop is generated by using dark-bright soliton conversion with wavelength center at $\lambda_0 = 1.50\,\mu m$, pulse width 35 fs and input data logic "0" (D) and logic "1" (B), when the input data logic "01" is added, the obtained output optical logic is "0101". When the input data logic "10" is added, the output optical logic "1010" is obtained. When the input data logic "11" is added, the output optical logic "0110" is obtained at through and drop ports T1, D1, D2, T2 respectively. The outputs can be used to perform the optical S-R flip-flop at drop ports D1 is $\overline{Q}_{n+1}$ and D2 is Q_{n+1} respectively.

Chapter 5

Conclusion

5.1 Conclusion

The significantly simple systems of basic optical gates based on dark-bright soliton conversion control technique have been proposed in this thesis. The concept of dark-bright soliton conversion control via the modified add-drop filter can be used to perform the logic operations in form of optical signal processing i.e. optical logic gates and optical S-R flip-flop. The proposed systems can be applied for ultrahigh speed memory or signal processing applications. In which the data logic status results can be simultaneously seen at the through ports and drop ports of the systems respectively.

The designed systems for optical S-R flip-flop is composed of two optical add/drop filters for performing the dark-bright soliton conversion concept, two BSs are integrated to separate the output in two light beams for the feedback signal and the output Q and Q, two BCs are used to combine the feedback light beams and the input beams. And the EDFA is used to manage the input and output power. Such all devices can be integrated in to a single system. Therefore, the proposed design system can be used for logical circuit which is recognized as the simple and flexible system for performing the logic switching system.

In addition, such devices can be extended and implemented for many flip-flop operations i.e. S-R, D, T and J-K flip-flop by a proper incorporation of dark-bright soliton conversion control based optical switches, which can be available for more advanced applications.

5.2 Future Works

In this thesis, the schematic of the optical logic gates or the optical S-R flip-flop based on the combination of add/drop filters. The architecture of the add/drop filter will obtained the results with the losses occurred in the filter at two points i.e., the loss of the couplings and dropping signal to the drop ports. To solve such problems, the architecture needs to change the material or device, and the replacement device much propertied as a waveguide with two channels receivers for the minimal loss. For the future plan in near future, in the new design system for performing optical logic operations, the most important is reducing loss incurred in add/drop device will be discussing, and the minimum loss transmission system will be design, the experiment for other logics such S-R, D, T and J-K flip-flops are also implemented.

APPENDIX

References

[1] Roy, J. N. And D. K. Gayen, "Integrated all-optical logic and arithmetic operations with the help of a TOAD-based interferometer device-alternative approach", Appl. Opt., Vol. 46, No. 22, 5304-5310, 2007.

[2] D. K. Maity, T. Chattopadhyay, D. K. Gayen, C. Taraphdar, A. K. Maiti, S. P. Maity, J. N. Roy, "All-optical binary flip-flop with the help of terahertz optical asymmetric demultiplexer", Nat. Comput., 9, 903-916 (2010).

[3] Han, B. C., J. L. Yu, W. R. Wang, L. T. Zhang, H. Hu, and E. Z. Yang, "Experimental study on all-optical half-adder based on semiconductor optical amplifier," Optoelectron. Lett., Vol. 5, No. 3, 0162-0164, 2009.

[4] D. Song, V. Gauss, H Zhang, M. Gross, P. Wen, S. Esener, "All-optical flip-flop based on vertical cavity semiconductor optical amplifiers", Opt. Lett., 32, 2969 - 2971 (2007).

[5] Khorasaninejad, M. and S. S. Saini, "All-optical logic gates using nonlinear effects in silicon-on insulator waveguides", Appl. Opt., Vol. 48, No. 25, F31-F36, 2009.

[6] Miyoshi, Y., K. Ileda, H. Tobioka, T. Inoue, S. Namiki, and K. I. Kitayama, "Ultrafast all-optical logic gates using nonlinear optical loop mirror based multi-periodic transfer function", Opt. Express, Vol. 16, No. 4, 2570-2577, 2008.

[7] Wang, J., Q. Sun, and J. Sun, "All-optical 40 Gbit/s CSRZ-DPSK logic XOR gate and format conversion using four-wave mixing", Opt. Express, Vol. 17, No. 15, 12555-12563, 2009.

[8] Wu, Y. D. and T. T. Shih, "New all-optical logic gates based on the local nonlinear mach-zehnder interferometer", Opt. Express, Vol. 16, No. 1, 248-257, 2008.

[9] Y. D. Jeong, J. S. Cho, Y. H. Won, "All-optical flip-flop based on the bistability of injection locked Fabry-Perot laser diode", Opt. Exp., 14, 4058-4063 (2006).

[10] E. Tangdiongga, X. Yang, Z. Li, Y. Liu, D. Lenstra, G. D. Khoe, H. J. S. Dorren, "Optical flip-flop based on two-coupled mode-locked ring lasers", IEEE Photon. Technol. Lett., 17, 208-210 (2005).

[11] Zhang, Y., Y. Zhang, and B. Li, "Optical switches and logic gates based on self-collimated beams in two-dimensional photonic crystals", Opt. Express, Vol. 15, No. 15, 9287-9292, 2007.

[12] A. Shinya, S. Mitsugi, T. Tanabe, M. Notomi, I. Yokohamma, "All-optical flip-flop circuit composed of coupled two-port resonant tunneling filter in two-dimensional photonic crystal slab", Opt. Express., 14, 1230–1235 (2006).

[13] C. H. Chen, S. Matsuo, K. Nozaki, A. Shinya, T. Sato, Y. Kawaguchi, H. Sumikura, M. Notomi, "All-optical memory based on injection-locking bistability in photonic crystal lasers", Optics Exp., 19 (4), 3387 -3395 (2011).

[14] K. Huybrechts, R. Baets, G. Morthier, "All-optical flip-flop operation in a standard tunable DBR laser diode", IEEE Photon. Technol. Lett., 21(24), 1873-1875 (2009).

[15] F. Ramos, E. Kehayas, J. M. Martinez, R. Clavero, J. Marti, L. Stampoulidis, D. Tsiokos,H. Avramopoulos, J. Zhang, P. V. Holm-Niesen, N. Chi, P. Jeppersen, N. Caenegem, D. Colle, M. Pickavet, and B. R. Ti, "IST-LASAGNE: Towards all-optical label swapping employing optical logic gates and optical flip-flops", IEEE Light. Tech., 23, 2993-3011 (2005).

[16] M. T. Hill, A. Srivatsa, N. Calabretta, Y. Liu, H. d. Waardt, G. D. Khoe, and H. J. S. Doren, "1x2 optical packet switch using all-optical header processing", Electron. Lett., 37, 774-775 (2001).

[17] P. P. Absil, J. V. Hryniewicz, B. E. Little, F. G. Johnson, P.-T. Ho, "Vertically coupled microring resonators using polymer wafer bonding," IEEE Photon. Technol. Lett., 13, 49-51 (2001).

[18] K. Sarapat, N. Sangwara, K. S rinuanjan, P. P. Yupapin, "Novel dark-bright optical solitons conversion system and power amplification," Opt. Eng. 48 (4), 045004-7 (2009).

[19] S. Mitatha, "Dark soliton behaviors within the nonlinear micro and nanoring resonators and applications", Progress In Electromagnetics Research, 99, 383-404 (2009).

[20] E. Rumelhart, J. L. McClelland, Eds., "Parallel distributed processing: Explorations in the microstructure of cognition", Vols. (1) (2), MIT Press, Boston (1986).

[21] S. Mukhopadhyay, J. N. Roy, S. K. Bera, "Design of minimized LED array for maximum parallel logic operations in optical shadow casting technique", Opt. Commun., 99, 31-37 (1993).

[22] T.Threepak, S. Mitatha and P.P. Yupapin , "Novel all-optical logic gate using an add drop filter and intensity switch", IEEE International Nano Electronic Conference 2010 (INEC2010) , City University of Hongkong, Kowloon , Hong Kong, January 3-8, 2010.

[23] Robert W. Boyd, Nonlinear optics, vol. 2. Academic Press, 2002.

[24] Kim, A. D., W. L. Kath, and C. G. Goedde, "Stabilizing dark solitons by periodic phase-sensitive amplification," Opt. Lett.,Vol. 21, 465, 1996.

[25] Su, Y., F. Liu, and Q. Li, "System performance of slow-light buffering and storage in silicon nano waveguide," Proc. SPIE,Vol. 6783, 68732, 2007.

[26] Christodoulides, D. N., T. H. Coskun, M. Mitchell, Z. Chen, and M. Segev, "Theory of incoherent dark solitons," Phys. Rev. Lett.,Vol. 80, 5113, 1998.

[27] Malomed, B. A., A. Mostofi, and P. L. Chu, "Transformation of a dark soliton into a bright pulse," J. Opt. Soc. Am. B, Vol. 17, 507, 2000.

[28] Fietz, C. and G. Shvets, "Nonlinear polarization conversion using microring resonators," Opt. Lett., Vol. 32, 1683, 2007

[29] Ballav, M. and A. R. Chowdhury, "On a study of diffraction and dispersion managed soliton in a cylindrical media," Progress In Electromagnetics Research, PIER 63, 33-50, 2006.

[30] E. Iannone, F. Matera, A. Mecozzi, and M. Settembre, Nonlinear Optical Communication Networks, 1998, pp. 35-36

[31] N. V. Alekseeva, K. N. Alekseev, V. A. Balueva, G. P. Berman, A. K. Popov and V. Z. Yakhnin "Optical chaos in multiple degenerate four-wave mixing," Journal Optical and Quantum Electronics, vol. 23, 1991, pp. 603-611

[32] Kumar V. Peddanarappagari and Maıté Brandt-Pearce, "Volterra series transfer function of single-mode fibers," Journal of lightwave Technology, vol. 15, 1997, pp. 2232-2241

[33] A. R. Chraplyvy, "Limitations of lightwave communications imposed by optical fiber nonlinearities," Journal of Lightwave Technology, vol. 8,1990, pp. 1548-1557

[34] P. P. Yupapin, P. Saeung and W. Suwancharoen, "Coupler-loss and coupling-coefficient dependence of bistability and instability in a fiber ring resonator:. nonlinear behaviors", Journal of Nonlinear Optical Physics and Materials, Volume 16, 2007, pp. 111-118

[35] S. Blair. " Optical soliton-based logic gates." Ph.D. dissertation, University of Colorado, 1998

[36] E. Infeld and G. Rowlands. " Nonlinear waves solitons and chaos. " Cambridge university press, 2000

[37] Agarwal, G. P., Nonlinear fiber optics, 4th Edition, Academic Press, New York, 2007.

[38] Hasegawa, Ed., A., Massive, WDM and TDM Soliton Transmission Systems, Kluwer Academic Publishers, 2000.

[39] Simonov, Yu. A. and J. A. Tjon, "Soliton-soliton interaction in confining models", Phys. Lett. B, Vol. 85, 380{384, 1979.

[40] Drohm, J. K., L. P. Kok, Yu. A. Simonov, J. A. Tjon, and A. I. Veselov, "Collision, and rotation of solitons in three space-time dimensions," Phys. Lett. B, Vol. 101, 204-208, 1981.

[41] Iizuka, T. and Yu. S. Kivshar, "Optical gap solitons in nonresonant quadratic media," Phys. Rev. E, Vol. 59, 7148-7151, 1999.

[42] Ganapathy, R., K. Porsezian, A. Hasegawa, and V. N. Serkin, "Soliton interaction under soliton dispersion management", IEEE J. Quantum Electron., Vol. 44, 383-390, 2008.

[43] E. A. J. Marcatili. "Bends in optical dielectric guides" ,Bell. Syst. Tech. J., vol. 48, September1969. pp. 2103-2132.

[44] E. A. J. Marcatili. "Dielectric rectangular waveguide and directional coupler for integrated optics", Bell. Syst. Tech. J., vol. 48, September 1969. pp. 2071-2101.

[45] Y. Ma, G. Chang, S. Park, L. Wang and S. T. Ho. 2000. "InGaAsP thin-film microdisk resonators fabricated by polymer wafer bonding for wavelength add-drop filters." 1495–1497. in IEEE Photonic Tech. L. Vol. 12.

[46] D. Rafizadeh et al.. "Waveguide-coupled Al GaAs/GaAs microcavity ring and disk resonators with high finesse and 21.6 nm free spectral range." Opt. Lett ., vol. 22, no. 16, August 1997. pp. 1244-1246.

[47] V. Van, T.A. Ibrahim, P.P. Absil, F.G. Jhonson, R. Grover and P.T. Ho. 2002. "Optical signal processing using nonlinear semiconductor micro ring resonators." 705-709. in IEEE J. Quantum Elect. Vol. 8.

[48] C. K. Madsen and J. H. Zhao. "A general planar waveguide autoregressive optical filter", IEEE J. Lightwave Tech., vol. 14, no. 3, March 1996. pp. 437-447.

[49] S. C. Hagness et al.. "FDTD microcavity simulations: design and experimental realization of waveguide-coupled single-mode ring and whispering-gallery-mode disk resonators", IEEE J. Lightwave Tech., vol. 15, no. 11, November 1997. pp. 2145-2165

[50] B. E. Little et al.. "Ultra-Compact Si-SiO2 microring resonator optical channel dropping filters", IEEE Photon. Techn. Lett ., vol. 10, no. 4, April 1998. pp. 549-551.

[51] D. J. W. Klunder et al., "Vertically and laterally waveguide-coupled cylindrical microresonators in Si3N4 on SiO2 technology." Appl. Phys. B 73, November 2001, pp. 603-608.

[52] B. Vanderhaegen et al. "High Q GaInAsP ring resonator filters." ECIO'99, Torino Italy, April 1999. pp. 381-384.

[53] M. K. Chin et al., "GaAs microcavity channel-dropping filter based on a race-track resonator", IEEE Photon. Techn. Lett ., vol. 11, no. 12, December 1999. pp. 1620-1622.

[54] N. Peyghambarian, H. M. Gibbs, "Optical bistability for optical signal processing and computing," Opt. Eng. 24(1), 68-72 (1985).

[55] N. Pahari, D. N. Das, S. Mukhopadhyay, "All-optical method for the addition of binary data by nonlinear materias," Appl. Opt., 43(33), 6147 -6150 (2004).

[56] C. R. Giles, Member, Ieee, E. Desurvire, J. R. Talman, J. R. Simpson, P. C. Becker, "2-Gbit/s signal amplification at $\lambda = 1.53\ \mu m$ in an erbium-doped single-mode fiber amplifier", Journal of lightwave Technology, vol. 7, Apr. 1989, pp. 651-656.

[57] F. J. Fraile-Pelaez, J. Capmany and M. A. Muriel, "Low threshold optical differential amplification using a fibre amplifier in a nonlinear ring resonator", Electronics Letters, vol. 29, 8 July 1993, pp. 1249-1251.

[58] S. Mitatha, N. Pornsuwancharoen, and P. P. Yupapin, "A simultaneous short-wave and millimeter-wave generation using a soliton pulse within a nano-waveguide", Photonics Technology Letters, IEEE, vol. 21, July1 2009, pp. 932-934.

List of Publications

1) Suphanchai Punthawanunt, **Saysamone Soysouvanh**, Khanthanou Luangxaysana, Somsak Mitatha, Masahiro Yoshida, Noriyuki Komine, and Preecha P. Yupapin, "THz Switching Generation Using a PANDA Ring Resonator for High Speed Computer Communication", PIERS Proceedings, 173-176, March 27-30, Kuala Lumpur, MALAYSIA 2012.

2) **Saysamone Soysouvanh**, Prapas Phongsanam, Khanthanou Luangxaysana, Somsak Mitatha, Noriyuki Komine, Masahiro Yoshida, and Preecha P. Yupapin, "All Optical Logic NAND Gate Using Dark-Bright Soliton Conversion Control", PIERS Proceedings, 177 - 180, March 27-30, Kuala Lumpur, MALAYSIA 2012.

3) **S. Soysouvanh**, K. Luangxaysana, P. Phongsanam, S. Mitatha, M. Yoshida, N. Komine, and P.P. Yupapin, "All-Optical S-R Flip-Flop using Dark-Bright Soliton Conversion Control", IEEE Proceedings, May 16-18, Hua Hin, THAILAND 2012.

4) Khanthanou Luangxaysana, **Saysamone Soysouvanh**, Prapas Phongsanam, Somsak Mitatha, Masahiro Yoshida, Noriyuki Komine, Yusaku Fujii and Preecha Yupapin, "High Capacity Optical Logic NAND Gate using a PANDA Ring Resonator System", July 15-18, Sapporo, JAPAN 2012.

All Optical Logic NAND Gate Using Dark-Bright Soliton Conversion Control

Saysamone Soysouvanh[1,2], Prapas Phongsanam[2], Khanthanou Luangxaysana[1,2], Somsak Mitatha[2], Komine Noriyuki[3], Masahiro Yoshida[3], and Preecha Yupapin[4]

[1]International College, King Mongkut's Institute of Technology Ladkrabang, Bangkok 10520, Thailand
[2]Hybrid Computing Research Laboratory, Faculty of Engineering
King Mongkut's Institute of Technology Ladkrabang, Bangkok 10520, Thailand
[3]School of Information and Telecommunication Engineering, Tokai University, Japan
[4]Nanoscale Science and Research Alliance (N'SEAR), Faculty of Science
King Mongkut's Institute of Technology Ladkrabang, Bangkok 10520, Thailand

Abstract— In this paper, we present a new concept of all-optical gates using Dark-Bright soliton conversion behaviors within a modified add/drop filter. The soliton can be used to generate logic data "1" and "0" using for optical gates. We have designed a photonic circuit for all-optical logic NAND Gate using dark-bright soliton conversion control within an optical add-drop multiplexer. The input and control logic '0', '1' are represented by dark (D) and bright (B) soliton pulses, respectively. We found that the simultaneous optical logic NAND Gate at the through port can be performed.

1. INTRODUCTION

The optical logic gates is one of the key techniques in all-optical signal processing and communication network, in which the implementation of all-optical logic gates can be used in various methods for processing signals with light. Many research have demonstrated various optical logic function using different schemes, such as including thermo-optic effect in two cascaded micro-ring resonators [1], quantum dot [2], semiconductor optical amplifier (SOA) [3–5], a terahertz optical asymmetric de-multiplex (TOAD) [6], nonlinear effects in SOI waveguide [7], nonlinear loop mirror [8], DPSK format [9], local nonlinear in MZI [10], photonic crystal [11]. Therefore, the searching for new design has become the interesting work. In this paper, we propose the one of the most important two logic gates namely NAND Gate based on dark-bright soliton conversion within the add/drop optical filter systems, which is a simple and flexible scheme for use as an arbitrary logic switching system. This can be used to form the advanced complex logic circuits, which will be detailed in the next section.

2. DARK-BRIGHT SOLITON CONVERSION

In operation, a ring resonator optical channel dropping filter (OCDF) is composed of two sets of coupled wave guides as shown in Figs. 1(a) and 1(b). For convenience, Fig. 1(a) is replaced by Fig. 1(b). The coupling equation outlined in the referenced in the previous section shows that there is a relative phase of $\pi/2$ between the signal coupled into the ring and the signal in the input bus.

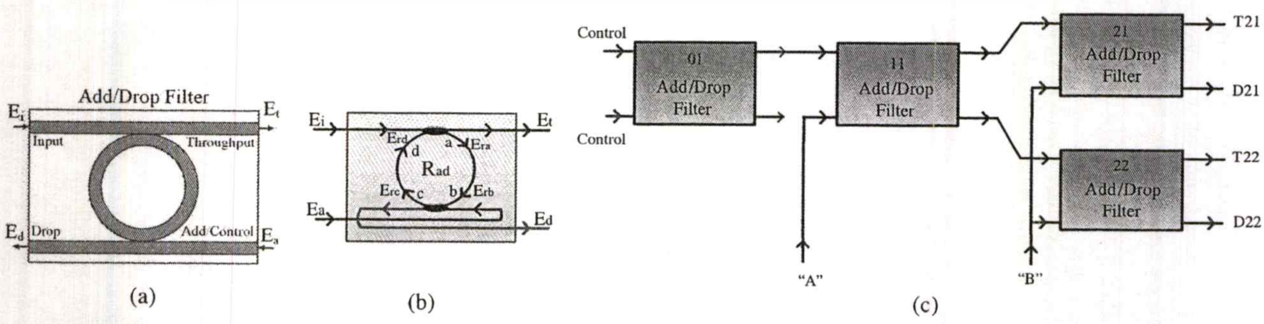

Figure 1: Schematic diagram simultaneous NAND Gate.

Similarly, the signal coupled into the drop and through ports, where both are acquired a phase of π with respect to the signal on the input port. This means that if we engineer the coupling coefficients appropriately, the field coupled into the through port on resonance would completely extinguish the resonant wavelength, and all power would be coupled into the drop port field.

$$E_{ra} = -jk_1E_i + \tau_1E_{rd} \tag{1}$$
$$E_{rb} = \exp(j\omega T/2)\exp(-\alpha L/4)E_{ra} \tag{2}$$
$$E_{rc} = \tau_2E_{rb} - jk2Ea \tag{3}$$
$$E_{rd} = \exp(j\omega T/2)\exp(-\alpha L/4)E_{rc} \tag{4}$$
$$E_t = \tau_1E_i - jk_1E_{rd} \tag{5}$$
$$E_d = \tau_2E_i - jk_2E_{rb} \tag{6}$$

here E_i is the input field, E_a is the added (control) field, E_t is the throughput field, E_d is the dropped field, $E_{ra}\ldots E_{rd}$ are the fields in the ring at the point $a\ldots d$, K_1 is the field coupling coefficient between the input and the ring, K_2 is the field coupling coefficient between the ring and the output bus, L is the circumference of the ring ($2\pi R$), T is the time taken for one round trip, $T{=}Ln_{eff}/c$, and α is the power loss in the ring per unit length. We assume that lossless coupling, i.e., The output power/intensities at the drop port and through port are given by π.

$$|E_d|^2 = \left|\frac{-\kappa_1\kappa_2A_{1/2}\Phi_{1/2}}{1-\tau_1\tau_2A\Phi}E_i + \frac{\tau_2-\tau_1A\Phi}{1-\tau_1\tau_2A\Phi}E_a\right|^2 \tag{7}$$
$$|E_t|^2 = \left|\frac{\tau_2-\tau_1A\Phi}{1-\tau_1\tau_2A\Phi}E_i + \frac{-\kappa_1\kappa_2A_{1/2}\Phi_{1/2}}{1-\tau_1\tau_2A\Phi}E_a\right|^2 \tag{8}$$

here $A_{1/2} = \exp(aL/4)$ (the half-round-trip amplitude); $A = (A_{1/2})^2$, $\Phi_{1/2} = \exp(j\omega T/2)$ (is the half-round-trip phase contribution), and $\Phi = (\Phi_{1/2})^2$. (The input and control fields at the input and add ports are formed by the dark-bright optical soliton [10] as shown in Equations (9)–(10).

$$E_{in}(t) = A_0\tanh\left[\frac{T}{T_0}\right]\exp\left[\left(\frac{z}{2L_D}\right) - i\omega_0t\right] \tag{9}$$
$$E_{in}(t) = A_0\sec h\left[\frac{T}{T_0}\right]\exp\left[\left(\frac{z}{2L_D}\right) - i\omega_0t\right] \tag{10}$$

here A and z are optical field amplitude and propagation distance, respectively. T is soliton pulse propagation time in a frame moving at the group velocity $T = t - \beta_1 - z$ where β_1 and β_2 are the coefficients of the linear and second-order terms of Taylor expansion of the propagation constant. $L_D = T_0^2/|\beta_2|$ is the dispersion length of the soliton pulse. T_0 in the equation is the initial soliton pulse width, where t is the soliton phase shift time, and the frequency shift of the soliton is ω_0. This solution describes a pulse that keeps its temporal width invariance as it propagates, and thus is called a temporal soliton. When a soliton peak intensity β/T_0^2 is given, then T_0 is known. For the soliton pulse in the nanoring device, a balance should be achieved between the dispersion length (L_D) and nonlinear length $L_{NL} = 1/\Gamma\phi_{NL}$, where $\Gamma = n_2k_0$, is the length scale over which dispersive or nonlinear effects make the beam become wider or narrower. For a soliton pulse, there is a balance between dispersion and nonlinear lengths, hence $L_D = L_{NL}$.

When light propagates within the nonlinear material (medium), the refractive index (n) of light within the medium is given by

$$n = n_0 + n_2I = n_0 + (n_2/A_{eff})P \tag{11}$$

here n_0 and n_2 are the linear and nonlinear refractive indexes, respectively. I and P are the optical intensity and optical power, respectively. The effective mode core area of the device is given by A_{eff}. For the micro/nano ring resonator, the effective mode core areas range from 0.50 to 0.10 μm^2. The resonant output of the light field is the ratio between the output and input fields [$E_{out}(t)$ and $E_{in}(t)$] in each round trip.

3. SIMULTANEOUS ALL-OPTICAL LOGIC GATES OPERATION

The proposed all-optical logic NAND Gate device is as shown in Fig. 1(b). The input and control light pulse trains are input in to the first add/drop optical filter (No. "01") using the dark-bright

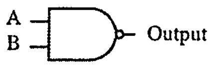

Input A	Input B	Output
0	0	1
0	1	1
1	0	1
1	1	0

Figure 2: Truth table NAND Gate.

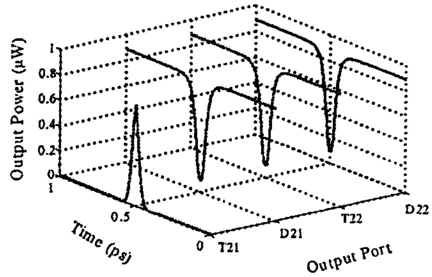

Figure 3: Show the output logic gates when the input logic stages 'DD'.

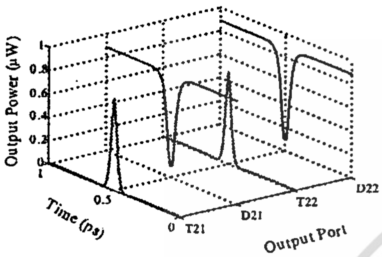

Figure 4: Show the output when the input logic stages 'DB'.

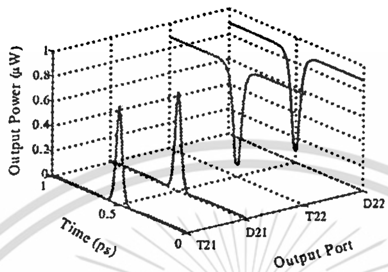

Figure 5: Show the output when the input logic stages 'BD'.

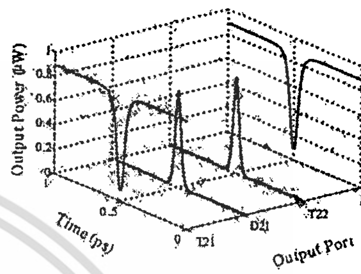

Figure 6: Show the output when the input logic stages 'BB'.

solitons, where firstly, the dark soliton is converted to be dark and bright solitons via the add/drop optical filter, which can be seen at the through and drop ports with π phase shift [12], respectively. By using the add/drop optical filters (No. "11", "12"), both input signals are generated by the first stage add/drop optical filter. Next, the input data "A" with logic "0" (dark soliton) and logic "1" (bright soliton) are added into both add ports. Secondly, the dark-bright soliton conversion with π phase shift is operated again. Finally, by using the add/drop optical filter (No. "21" to "22"), the input data "B" with logic "0" (dark soliton) and logic "1" (bright soliton) are seen at all the add ports. For large scale (Fig. 1(c)), results obtained are simultaneously seen by D21, D22, T22, T21 at the drop and through ports for optical logic gates, respectively. The truth table of NAND Gate is as shown in Fig. 2.

In simulation, the add/drop optical filter parameters are fixed for all coupling coefficients to be $K_s = 0.05$, $R_{ad} = 1.51\,\mu m$, $A_{eff} = 0.25\,\mu m^2$, $a = 0.05\,dBmm^{-1}$, $\gamma = 0.01$, $n_{eff} = 3.14$ $(forGaAsP/InP)$ for all add/drop optical filters in the system. Result of the all-optical NAND gate is generated by using dark-bright soliton conversion with wavelength center at $\lambda_0 = 1.50\,\mu m$, pulse width 35 fs and input data logic "0" (dark soliton) and logic "1" (bright soliton). When the input data logic "00" is added, the obtained output optical logic is "1000" [Fig. 3]. When the input data logic "01" is added, the output optical logic "1010" [Fig. 4] is obtained. When the input data logic "10" is added, the output optical logic "1100" [Fig. 5] is obtained. When the input data logic "11" is added, we found that the output optical logic "0110" [Fig. 6] is seen.

We found that output data logic at the through port T21 is optical logic NAND Gate, the output data logic at drop port D21 and through port T22 are same with the input A and B respectively.

4. CONCLUSION

We have shown that the proposed photonic circuit can be used to create the logic NAND Gate. With the input data logic "0" (dark soliton) and logic "1" (bright soliton), the all-optical device can perform the optical logic NAND at the T21 output. This could be a potential key component in the all-optical signal processing, which is a simple and flexible scheme that can be used to perform the advanced logic switching system. This can be extended and implemented for any higher number of input digits by the proper incorporation of dark-bright soliton conversion control, based optical switches.

ACKNOWLEDGMENT

We would like to acknowledge to the Asian University Network (AUN/SEED-Net) for the financial support of one of the authors (Mr. Saysamone Soysouvanh) from National University of LAOS (NUOL), LAO PDR for his graduate study at King Mongkut's Institute of Technology Ladkrabang (KMITL), Thailand.

REFERENCES

1. Zhang, L., R. Ji, L. Jia, L. Yang, P. Zhou, Y. Tian, P. Chen, Y. Lu, Z. Jiang, Y. Liu, Q. Fang, and M. Yu, "Demonstration of directed XOR/XNOR logic gates using two cascaded microring resonators," *Opt. Lett.*, Vol. 35, No. 10, 1620–1622, 2010.
2. Ma, S., Z. Chen, H. Sun, and K. Dutta, "High speed all optical logic gates based on quantum dot semiconductor optical amplifiers," *Opt. Express*, Vol. 18, No. 7, 6417–6422, 2010.
3. Dong, J., X. Zhang, and D. Huang, "A proposal for two-input arbitrary Boolean logic gates using single semiconductor optical amplifier by picoseconds pulse injection," *Opt. Express*, Vol. 17, No. 10, 7725–7730, 2009.
4. Dong, J., X. Zhang, J. Xu, and D. Huang, "40 Gb/s all-optical logic NOR and OR gates using a semiconductor optical amplifier: Experimental demonstration and theoretical analysis," *Opt. Commun.*, Vol. 281, 1710–1715, 2008.
5. Han, B. C., J. L. Yu, W. R. Wang, L. T. Zhang, H. Hu, and E. Z. Yang, "Experimental study on all-optical half-adder based on semiconductor optical amplifier," *Optoelectron. Lett.*, Vol. 5, No. 3, 0162–0164, 2009.
6. Roy, J. N. and D. K. Gayen, "Integrated all-optical logic and arithmetic operations with the help of a TOAD-based interferometer device-alternative approach," *Appl. Opt.*, Vol. 46, No. 22, 5304–5310, 2007.
7. Khorasaninejad, M. and S. S. Saini, "All-optical logic gates using nonlinear effects in silicon-on insulator waveguides," *Appl. Opt.*, Vol. 48, No. 25, F31–F36, 2009.
8. Miyoshi, Y., K. Ileda, H. Tobioka, T. Inoue, S. Namiki, and K. I. Kitayama, "Ultrafast all-optical logic Gates using n nonlinear optical loop mirror based multi-periodic transfer function," *Opt. Express*, Vol. 16, No. 4, 2570–2577, 2008.
9. Wang, J., Q. Sun, and J. Sun, "All-optical 40 Gbit/s CSRZ-DPSK logic XOR gate and format conversion using four-wave mixing," *Opt. Express*, Vol. 17, No. 15, 12555–12563, 2009.
10. Wu, Y. D. and T. T. Shih, "New all-optical logic gates based on the local nonlinear Mach-Zehnder interferometer," *Opt. Express*, Vol. 16, No. 1, 248–257, 2008.
11. Zhang, Y., Y. Zhang, and B. Li, "Optical switches and logic gates based on self-collimated beams in two-dimensional photonic crystals," *Opt. Express*, Vol. 15, No. 15, 9287–9292, 2007.
12. Kokubun, Y., Y. Hatakeyama, M. Ogata, S. Suzuki, and N. ZaiZen, "Fabrication technologies for vertically coupled microring resonator with multilevel crossing busline and ultracompact-ringradius," *IEEE J. Sel. Top. Quantum Electron.*, Vol. 11, 4–10, 2005.

All-Optical S-R Flip-Flop using Dark-Bright Soliton Conversion Control

S. Soysouvanh, P. Phongsanam, K. Luangxaysana, S. Mitatha, M. Yoshida, N. Komine and P.P. Yupapin

S. Soysouvanh, K. Luangxaysana
International College
Hybrid Computing Research Laboratory
Faculty of Engineering
King Mongkut's Institute of Technology Ladkrabang
Bangkok, 10520 Thailand
E-mail: l-khun@hotmail.com, khanthanou@live.com

M. Yoshida, N. Komine
Department of Embedded Technology
School of Information and Telecommunication Engineering
Tokai University, Japan

P. Phongsanam, S. Mitatha
Hybrid Computing Research Laboratory
Faculty of Engineering
King Mongkut's Institute of Technology Ladkrabang
Bangkok, 10520 Thailand
E-mail: ctr_alt_del@hotmail.com

P.P. Yupapin
Nanoscale Science and Engineering Research Alliance,
Faculty of Science
King Mongkut's Institute of Technology Ladkrabang
Bangkok 10520, Thailand

***Abstract*—We propose a new design for all-optical S-R flip-flop using optical technique namely dark-bright soliton conversion control within an optical add-drop filter. In operation, all-optical data input logic '0', '1' is formed by dark soliton (D) and bright soliton (B) pulses, respectively. The conversion behaviour between dark and bright soliton pulses can be obtained and formed the logic pulses by a $\pi/2$ phase shifted device (i.e. an optical coupler), in which the binary logic operation can be formed simultaneously at the thought and drop ports, respectively. In all-optical S-R flip-flop application can be recognized as a simple and flexible system for forming the logic switching system. Numerical simulation results are obtained and confirmed for the useful application, in which the advanced logical system can be operated.**

Keywords-all-optical flip-flop; Digital optics; Add-drop filter

I. INTRODUCTION

To date, the studies of optical techniques have been widely increasing and applying for many optical applications for communication use. One of those applications is a processing system. An all-optical flip-flop is the packet switches in the next generation of communication network. The flip-flop is a logic gates that maintain a stable state output even after the input is turned off, in which the key basic function is represented by the logic gates (NOR, NAND). Nowadays, All-optical flip-flop is an essential component for latching functions in ultrahigh speed all-optical processing applications [1, 2]. Currently, many systems such as a terahertz optical asymmetric de-multiplex (TOAD) [3], semiconductor optical amplifier [4], Fabry-Perot laser diode [5], ring lasers [6], photonic crystals [7, 8], DBR laser diode [9] have been proposed. In this paper, we have presented an all-optical flip-flop system for logical processing operation, which can be replaced used for an electronic circuit [10-13] by using dark-bright soliton pulses conversion control [14, 15], the theoretical background is also reviewed. For our concept, the all-optical flip-flop operation of binary based on dark-bright solitons conversion behaviors can be performed, in which the coincidence dark and bright soliton pulses can be separated after propagating into the optical-filter device with $\pi/2$ phase shifted (an optical coupler) [14]. The proposed scheme is based on a 1 bit binary to the complex logic circuits, which can be compared by any 2 bits, when logic '0' and '1' are formed by dark and bright soliton pulses, respectively.

II. DARK-BRIGHT SOLITONS CONVERSION CONTROL

In the operation of dark-bright solitons conversion [16] using a ring resonator as shown in Fig. 1, where in this case the dark-bright solitons conversion system [17, 18] using an optical channel dropping filter (OCDF) [19-24] is composed of two set of coupled waveguide, as shown in Fig.1 (a) and Fig.1 (b), when for convenience, Fig. 1(b) is replaced by Fig. 1(a). The relative phase of the two output light signals after coupling into the optical coupler is $\pi/2$ before coupling into the ring and the input bus, respectively. This means that the signals coupled into the drop and through ports are acquired a phase of π with respect to the input port signal. In application, if the coupling coefficients are formed appropriately, the field coupled into the through port would completely extinguish the resonant wavelength, and all power would be coupled into the drop port, in which the dark-bright conversion behaviours are described by Eqs. (1) - (8).

$$E_{ra} = -jK_1E_i + \tau_1E_{rd}. \quad (1)$$

$$E_{rb} = exp(j\omega T/2)exp(-\alpha L/4)E_{ra}. \quad (2)$$

$$E_{rc} = \tau_2E_{rb} + jK_2E_{ra}. \quad (3)$$

AUN/SEED-Net, JICA

78-1-4673-2025-2/12/$31.00 ©2012 IEEE

$$E_{rd} = exp(j\omega T/2)exp(-\alpha L/4)E_{rc}. \quad (4)$$

$$E_t = \tau_1 E_i - jK_1 E_{rd}. \quad (5)$$

$$E_d = \tau_2 E_a - jK_2 E_{rb}. \quad (6)$$

Where E_i is the input field, E_a is the added (control) field, E_t is the throughput field, E_d is the dropped field, $E_{ra}...E_{rd}$ are the fields in the ring at the point $a...d$, K_1 is the field coupling coefficient between the input and the ring, K_2 is the field coupling coefficient between the ring and the output bus, L is the circumference of the ring ($2\pi R$), T is the time taken for one round trip, and α is the power loss in the ring per unit length. We assume that lossless coupling, i.e. $\tau_{1,2} = \sqrt{1-\kappa_{1,2}^2}$, T is the round-trip time $T = Ln_{eff}/c$. The output power-intensities at the drop port and through port are given by [21, 24].

$$|E_d|^2 = \left|\frac{-\kappa_1\kappa_2 A_{1/2}\Phi_{1/2}}{1-\tau_1\tau_2 A\Phi}E_i + \frac{\tau_2-\tau_1 A\Phi}{1-\tau_1\tau_2 A\Phi}E_a\right|^2 \quad (7)$$

$$|E_t|^2 = \left|\frac{\tau_2-\tau_1 A\Phi}{1-\tau_1\tau_2 A\Phi}E_i + \frac{-\kappa_1\kappa_2 A_{1/2}\Phi_{1/2}}{1-\tau_1\tau_2 A\Phi}E_a\right|^2 \quad (8)$$

Where $A_{1/2} = exp(-\alpha L/4)$ (the half-round-trip amplitude). $A = A_{1/2}^2$, $\Phi_{1/2} = exp(j\omega T/2)$...(the half-round-trip phase contribution), and $\Phi = \Phi_{1/2}^2$ .The input and control fields at the input and add ports are formed by the dark-bright optical solitons [12-13] as shown in Eqs. (9) – (10).

$$E_{in}(t) = A_0 \sec h\left[\frac{T}{T_0}\right]\exp\left[\left(\frac{z}{2L_D}\right) - i\omega_0 t\right] \quad (9)$$

$$E_{in}(t) = A_0 \tanh\left[\frac{T}{T_0}\right]\exp\left[\left(\frac{z}{2L_D}\right) - i\omega_0 t\right] \quad (10)$$

Where A and z are optical field amplitude and propagation distance, respectively. T is soliton pulse propagation time in a frame moving at the group velocity $T = t-\beta_1 z$, where β_1 and β_2 are the coefficients of the linear and second-order terms of Taylor expansion of the propagation constant. $L_D = T_0^2/|\beta_2|$ is the dispersion length of the soliton pulse. T_0 in the equation is the initial soliton pulse width, where t is the soliton phase shift time, and the frequency shift of the soliton is ω_0. This solution describes a pulse that keeps its temporal width invariance as it propagates, and thus is called a temporal soliton. When a soliton peak intensity $(\beta/\Gamma T_0^2)$ is given, then T_0 is known. For the soliton pulse in the nanoring device, a balance should be achieved between the dispersion length (L_D) and nonlinear length $L_{NL} = 1/\Gamma\phi_{NL}$), where $\Gamma = n2k0$, is the length scale over which dispersive or nonlinear effects make the beam become wider or narrower. For a soliton pulse, there is a balance between dispersion and nonlinear lengths, hence $L_D = L_{NL}$.

When light propagates within the nonlinear material (medium), the refractive index (n) of light within the medium is given by Eq. (11).

$$n = n_0 + n_2 I = n_0 + \frac{n_2}{A_{eff}}P \quad (11)$$

Here n_0 and n_2 are the linear and nonlinear refractive indexes, respectively. I and P are the optical intensity and optical power, respectively. The effective mode core area of the device is given by A_{eff}. For the micro/nano ring resonator, the effective mode core areas range from 0.10 to $0.50\ \mu m^2$ [6]. The resonant output of the light field is the ratio between the output and input fields [$Eout(t)$ and $Ein(t)$] in each round trip, which is given by references [16-18, 24].

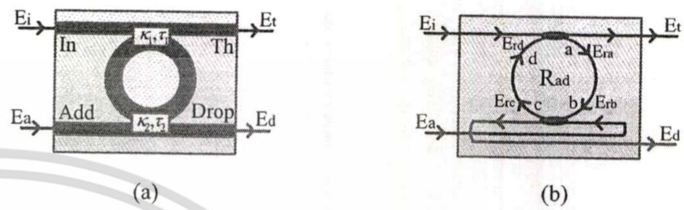

Figure 1. A schematic diagram of the dark-bright soliton conversion control system

III. ALL OPTICAL S-R FLIP-FLOP

S-R flip-flop is a circuit with two cross-coupled NOR gates or two cross-coupled NAND gate. It has two input signals, which one is S and the other is R for setting and resetting the outputs $\bar{Q}_{n+1}$ and Q_{n+1}, respectively. The S-R flip-flop outputs are the feedback signals. There are three status logic output signals, which is called "Hold" when no input signal (S = 0, R=0), "Set" when S=1 and R=0 and "Reset" when S=0, R=1, respectively. The proposed scheme for all-optical S-R flip-flop using beam splitter (BS) and beam combiner (BC) is as shown in Fig.2 (c). The input logic '1' is formed by bright soliton and logic '0' is formed by absence of the input signal. The other technique that can be used to form the similar operation is found in reference [12], in which the optical power signal is manipulated by erbium doped fiber amplifier (EDFA).

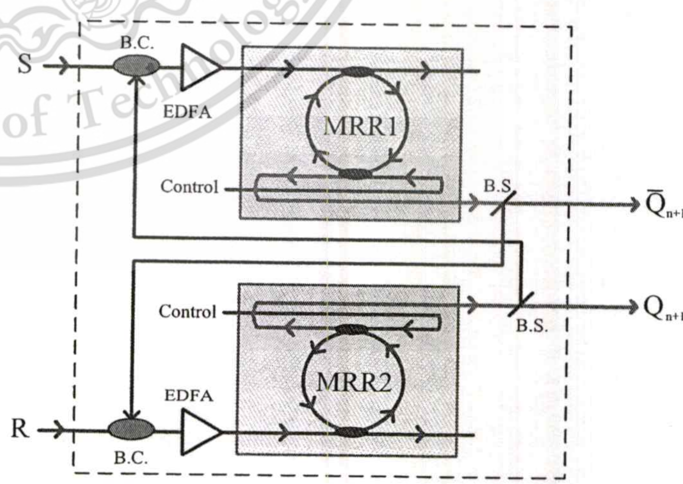

Figure 2. Schematic of S-R Flip-Flop

In simulation, the add/drop optical filter [25-27] parameters are used and fixed to be $K_s=0.5$, $Rad=1.55\mu m$, $A_{eff}=0.25\mu m^2$, $\alpha=0.05dBmm^{-1}$, $\gamma=0.01$, $n_{eff}=3.14$ (*for InGaAsP/InP*) for all add/drop optical filters in the system. Results of the all-optical flip-flop are generated by the dark-bright solitons conversion behaviors, with center wavelength is at $\lambda_0=1.50\mu m$, pulse width of *35fs* and the input data logic "0" and "1" are represented by the dark and bright soliton pulses, respectively. In Fig. 3, the simultaneous output optical logic is seen, which can be configured as following details.

Case 1: When it is no input signal, S = R = 0, where Q_{n+1} and $\overline{Q}_{n+1}$ are not changed. This state is called "Hold".

Case 2: By using the dark-bright solitons conversion behavior, when S = 0 and R = 1, the input logic '0' and '1' is formed by dark-bright solitons, where both input signals are converted to dark-bright soliton pulses with π phase shift. The detector D2 receives the logic '0' (dark soliton), i.e. $Q_{n+1}=0$, which is connected to the input 'S', then the dark-bright solitons conversion with π phase shift is operated again. When the detector D1 receives the logic '1' (bright soliton), hence $\overline{Q}_{n+1}=1$ [see Fig 3], in which Q_{n+1} and $\overline{Q}_{n+1}$ are connected to the input 'S' and 'R', respectively. Therefore, if both 'S' and 'R' are no input signals, i.e. S = R = 0. Then Q_{n+1} and $\overline{Q}_{n+1}$ are the feedback signals, which is called the "Reset".

Case 3: When S = 1 and R = 0, the logic '0' and '1' is formed by dark-bright solitons, where both input signals are converted to dark-bright solitons with π phase shift. When D1 receives the logic '0' (dark soliton) i.e. $\overline{Q}_{n+1}=0$, which is connected to the input 'R', then the dark-bright solitons conversion with π phase shift is formed. When the detector D2 receives the logic '1' (bright soliton), hence $Q_{n+1}=1$ [see Fig 4], where Q_{n+1} and $\overline{Q}_{n+1}$ are connected to the input 'S' and 'R', respectively. Therefore, if both 'S' and 'R' are no input signals, i.e. S=R=0. Then Q_{n+1} and $\overline{Q}_{n+1}$ are the feedback signals, which is called the "Set".

Case 4: When S = R = 1 then both MRR1 and MRR2 receive both the incoming bright soliton signals, i.e. $Q_{n+1}=\overline{Q}_{n+1}=1$ [see Fig 5], this state is called the "Forbidden".

The truth table for output of the one bit binary R-S Flip-Flop is concluded in Table: 1.

TABLE I. CONCLUSION OF THE BINARY S-R FLIP-FLOP

Input		Output		State
S	*R*	Q_{n+1}	$\overline{Q}_{n+1}$	
0	0	Q_n	$\overline{Q}_n$	Hold
0	1	0	1	Reset
1	0	1	0	Set
1	1	1	1	Forbidden

Logic '0' = 'Dark soliton, Logic '1' = 'Bright soliton'.

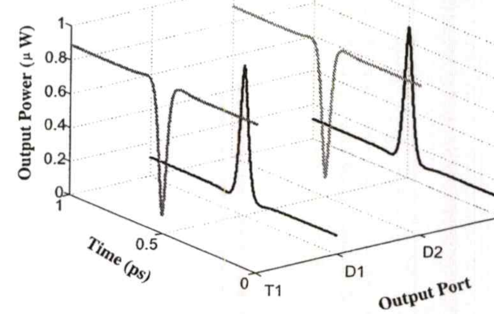

Figure 3. Show the output when 'Reset' stage.

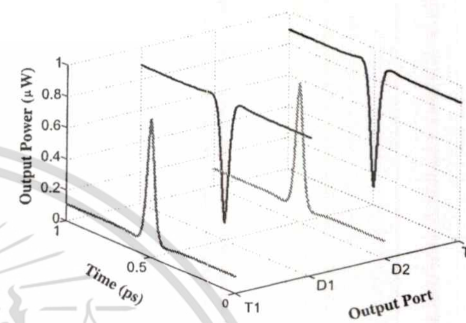

Figure 4. Show the output when 'Set' stage.

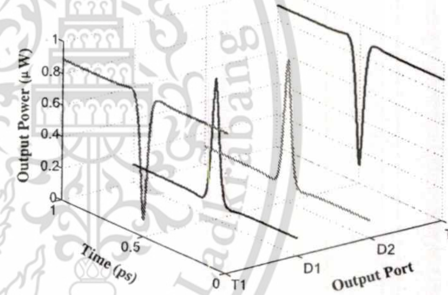

Figure 5. Show the output when 'Set' stage.

IV. CONCLUSION

We proposed new designed for basic all-optical flip-flop operations based on dark-bright solitons conversion control system via the modified add/drop filters for ultrahigh speed memory or signal processing application. Based on the dark-bright solitons conversion control concept, the data logic '0' (dark soliton) and '1' (bright soliton) using all-optical in nature can be used to form the flip-flop operations, in which the logic status results can be obtained simultaneously at the drop and through ports, respectively. Therefore, the proposed design can be used for logical circuit which is recognized as the simple and flexible system for performing the logic switching system. Moreover, such device can be extended and implemented for any flip-flop such as S-R, D, T and J-K flip-flop by a proper incorporation of dark-bright solitons conversion control based optical switches, which can be available for more advanced applications.

Acknowledgment

We would like to acknowledge to the Asian University network (AUN/SEED-Net) for the financial support of one of the authors (Mr. Saysamone Soysouvanh) from National University of LAOS (NUOL), LAO PDR for his graduate study at King Mongkut's Institute of Technology Ladkrabang (KMITL), Thailand.

References

[1] F. Ramos, E. Kehayas, J. M. Martinez, R. Clavero, J. Marti, L. Stampoulidis, D. Tsiokos,H. Avramopoulos, J. Zhang, P. V. Holm-Niesen, N. Chi, P. Jeppersen, N. Caenegem, D. Colle, M. Pickavet, and B. R. Ti, "IST-LASAGNE: Towards all-optical label swapping employing optical logic gates and optical flip-flops", IEEE Light. Tech., 23, 2993-3011 (2005)

[2] M. T. Hill, A. Srivatsa, N. Calabretta, Y. Liu, H. d. Waardt, G. D. Khoe, and H. J. S. Doren, "1x2 optical packet switch using all-optical header processing", Electron. Lett., 37, 774-775 (2001)

[3] D. K. Maity, T. Chattopadhyay, D. K. Gayen, C. Taraphdar, A. K. Maiti, S. P. Maity, J. N. Roy, "All-Optical binary Flip-Flop with the help of Terahertz Optical Asymmetric Demultiplexer," Nat. Comput., 9, 903-916 (2010).

[4] D. Song, V. Gauss, H Zhang, M. Gross, P. Wen, S. Esener, "All-optical flip-flop based on vertical cavity semiconductor optical amplifiers", Opt. Lett., 32, 2969- 2971 (2007)

[5] Y. D. Jeong, J. S. Cho, Y. H. Won , "All-optical flip-flop based on the bistability of injection locked Fabry-Perot laser diode", Opt. Exp., 14, 4058-4063 (2006).

[6] E. Tangdiongga, X. Yang, Z. Li, Y. Liu, D. Lenstra, G. D. Khoe, H. J. S. Dorren, "Optical flip-flop based on two-coupled mode-locked ring lasers", IEEE Photon. Technol. Lett., 17, 208-210 (2005).

[7] A. Shinya, S. Mitsugi, T. Tanabe, M. Notomi, I. Yokohamma, "All-optical flip-flop circuit composed of coupled two-port resonant tunneling filter in two-dimensional photonic crystal slab". Opt. Express., 14, 1230–1235 (2006)

[8] C. H. Chen, S. Matsuo, K. Nozaki, A. Shinya, T. Sato, Y. Kawaguchi, H. Sumikura, M. Notomi,"All-optical memory based on injection-locking bistability in photonic crystal lasers", Optics Exp., 19 (4), 3387-3395 (2011)

[9] K. Huybrechts, R. Baets, G. Morthier, "All-optical flip-flop operation in a standard tunable DBR laser diode," IEEE Photon. Technol. Lett., 21(24), 1873–1875 (2009)

[10] S. Mukhopadhyay, J. N. Roy, S. K. Bera, "Design of minimized LED array for maximum parallel logic operations in optical shadow casting technique," Opt. Commun., 99, 31-37 (1993).

[11] E. Rumelhart, J. L. McClelland, Eds., "Parallel Distributed Processing : Explorations in the Microstructure of Cognition," Vols. (1)(2), MIT Press, Boston (1986).

[12] N. Peyghambarian, H. M. Gibbs, "Optical bistability for optical signal processing and computing," Opt. Eng. 24(1), 68-72 (1985).

[13] N. Pahari, D. N. Das, S. Mukhopadhyay, "All-optical method for the addition of binary data by nonlinear materias," Appl. Opt., 43(33), 6147-6150 (2004).

[14] K. Sarapat, N. Sangwara,.K. Srinuanjan, P. P. Yupapin, "Novel dark-bright optical solitons conversion system and power amplification," Opt.Eng. 48(4), 045004-7 (2009).

[15] S. Mitatha, "Dark soliton behaviors within the nonlinear micro and nanoring resonators and applications," Progress In Electromagnetics Research, 99, 383-404 (2009).

[16] S. Mitatha, N. Chaiyasoonthorn, P. P. Yupapin, "Dark-bright optical solitons conversion via an optical add/drop filter," Microw. and Opt. Technol. Lett., 51, 2104-2107 (2009).

[17] T. Phatharaworamet, C. Teeka, R. Jomtarak, S. Mitatha, P. P. Yupapin, "Random Binary Code Generation Using Dark-Bright Soliton Conversion Control Within a PANDA Ring Resonator," IEEE Lightwave Technol., 28(19), 2804-2809 (2010).

[18] P. Juleang, P. Phongsanam, S. Mitatha, and P.P. Yupapin, "Public Key Suppression and Recovery using a PANDA Ring Resonator for High Security Communication," Opt. Eng., 52(3), 035002-1-6 (2011).

[19] P. P. Absil, J. V. Hryniewicz, B. E. Little, F. G. Johnson, P.-T. Ho, "Vertically coupled microring resonators using polymer wafer bonding," IEEE Photon. Technol. Lett., 13, 49-51 (2001).

[20] R. Grover, P. P. Absil, V. Van, J. V. Hryniewicz, B. E. Little, O. S. King, L. C. Calhoun, F. G. Johnson, P.-T. Ho, "Vertically coupled GaInAsP-InP microring resonators," Opt. Lett., 26, 506-508 (2001).

[21] V. Van, T. A. Ibrahim, P. P. Absil, F. G. Johnson, R. Grover, "Optical signal processing using nonlinear semiconductor micro ring resonators," IEEE J. of Sel. Top. in Quantum Electron., 8, 705-713 (2002).

[22] S. Mitatha, N. Pornsuwancharoen, P. P. Yupapin, "A simultaneous short-wave and millimeter-wave generation using a soliton pulse with in a nano-waveguide," IEEE Photon. Technol. Lett., 13, 932-934 (2009).

[23] P. P. Yupapin, N. Pornsuwancharoen, "Guided Wave Optics and Photonics: Micro Ring Resonator Design for Telephone Network Security," Nova Science Publishers, New York (2008).

[24] P.P. Yupapin, N. Pornsuwanchroen, S. Chaiyasoonthorn, "Attosecond pulse generation using nonlinear micro ring resonator," Microw. Opt. Technol Lett.,50, 3108-3011 (2008).

[25] Q. Xu, D. Fattal, R. G. Beausoleil, "Silicon microring resonators with 1.5-μm radius," Opt. Exp., 16(2008)4309-4315.

[26] J. Wang, Q. Sun, and J. Sun, "All-optical 40 Gbit/s CSRZ-DPSK logic XOR gate and format conversion using four-wave mixing," Opt. Express, 17(15), 12555-12563 (2009).

[27] S. Mookherjea, M. A. Schneider, "The nonlinear microring add-drop filter," Opt. Exp., 16, 15130-15136 (2008).

Author Biography

Name:	SAYSAMONE SOYSOUVANH
Date of Birth:	08 October 1989
Place of Birth:	Vientiane, Lao PDR
Address:	224, Phonepapao village, Sisattanak district, Vientiane Capital, Lao PDR
Education:	Bachelor Degree of Engineering in Computer Engineering from Faculty of Engineering, National University of Laos in 2010
Organization:	Department of Computer Engineering and Information Technology Faculty of Engineering, National University of Laos (NUOL)
Position:	Lecturer
Work Experiences:	1 semester for lecturer in the Department of Computer Engineering and Information Technology, Faculty of Engineering, National University of Laos
Research Field:	Optical Communication
Interesting Topic:	Computer Programming, Computer Networking, and Optical Communication.